liver and small bowel transplantation secondary to malabsorption and TPN induced cholestatic liver disease. Nearly one year after transplantation, at age 2y 10 mos, this patient expired from an apparent episode of sepsis. This patient did not yet demonstrate type 1 diabetes.

Design: An autopsy was performed with attention to the cause of death, identification of any qualitative gross developmental abnormalities, microscopic abnormalities, disorders of selected endocrine tissues, and a comparison of graft intestine with residual native intestine. Immunohistochemistry for various endocrine markers was performed. The pancreas was additionally studied for quantitative differences in endocrine development compared to age matched controls.

Results: The autopsy cultures revealed *E. coli* in the blood; *E. coli, K. pneumoniae*, and enterococcus species from the central line; and all the above plus *S. viridans* in the lungs. Chromogranin A immunohistochemistry identified endocrine cells in the pituitary, trachea, bronchi, stomach, graft small bowel, and pancreas. Endocrine cells of the residual native small bowel were not detected, and were only rarely found in the residual native colon. The pancreas demonstrated a markedly reduced number of islet cells.

Conclusions: The most likely cause of death was from line sepsis. The intestinal endocrine cell deficiency persisted in the native intestine and the deficiency did not occur in the transplanted intestine. The defective NEUROG3 resulted in an endocrine cell deficiency in the human pancreas.

23 Kidney Injury Molecule-1 Is a Specific Biomarker Which Enables Diagnosis of Pre-Mortem Acute Tubular Necrosis in the Presence of Autolytic Artifacts in Cadaver Kidneys

PL Zhang, F Lin, WK Han, TM Blasick, JV Bonventre. Geisinger Medical Center, Danville, PA; Brigham and Women's Hospital, Boston, MA.

Background: KIM-1 is a specific biomarker that can identify acute tubular necrosis (ATN) in native and transplant renal biopsies. In kidneys studied on autopsy it is usually difficult to differentiate ATN from renal autolysis. In this study we determined whether KIM-1 staining could identify pre-morbid ATN in cadaver kidneys, even when autolysis was present.

Design: Forty-three autopsy kidneys were stained by immunohistochemistry for KIM-1 with AKG-7 anti-KIM-1 monoclonal antibody. The staining intensity scores of KIM-1 along proximal tubular membranes (0 to 3+) were recorded and correlated with renal functional indices present prior to death. Phosphorylated (p)-mTOR and p-p70S6K (two downstream signals of growth factors) were also identified using immunohistochemical techniques.

Results: KIM-1 staining scores were significantly positively correlated with antemortem blood urea nitrogen (BUN, $r = 0.53$, $p < 0.003$) and serum creatinine ($r = 0.63$, $p < 0.0001$) and negatively correlated with estimated glomerular filtration rate ($r = 0.52$, $p < 0.0064$), despite prominent autolysis in one half of cases. Cases were divided into three groups: group 1 (multiple causes of death, n = 23); group 2 (acute myocardial infarction, n = 8); and group 3 (cirrhosis with liver failure, n = 12). Groups 2 and 3 had significantly higher scores of kidney KIM-1 staining when compared to group 1 ($p<0.05$). KIM-1 positive staining was found in 52%, 88% and 92% of kidneys in Groups 1, 2 and 3 respectively. Upregulated KIM-1 in injured proximal tubules was seen concurrently with enhanced expression of p-mTOR and p-p70S6K and membranous KIM-1 protein co-localized with translocated p-p70S6K in the nuclei by a double staining method.

Conclusions: Whether or not autolysis is present, KIM-1 expression is a specific biomarker for proximal tubular injury and is significantly correlated with renal dysfunction. KIM-1 may regulate the m-TOR-pp70S6K growth pathway. The high degree of KIM-1 expression in group 2 is consistent with a high degree of renal ischemia following myocardial infarction. In group 3, the high percent of positive KIM-1 staining suggests that liver disease is often associated with ATN and not purely a functional kidney defect.

24 An Analysis of Pediatric Autopsy Findings through Text Mining

Z Zuo, EA Manci. University of South Alabama, Mobile, AL.

Background: Few collective analyses of pediatric autopsies are in literature. This study aims to a better understanding of the etiology in pediatric deaths.

Design: Retrospective review of pediatric autopsies performed during November 1996 to March 2006 at our Children's And Women's Hospital. Autopsy reports were programmatically extracted from LIS and parsed into relational database for statistics by text mining using Visual Basic and SQL. A structured report template of our department enabled text mining to successfully retrieve relevant information from reports. All text mining results were manually verified.

Results: 228 pediatric autopsies were found in the reviewed period, with decreasing numbers performed each year since 1999. 125 cases occurred as intrauterine fetal demise (IUFD). The male/female ratio was 136/92 in all deaths, and 71/54 in IUFD. While sepsis still the most common etiology, it has declined from 72.5% in 1997 to 22.2% in 2005. Among congenital diseases, 5 were Turner's syndrome, all IUFD around 2nd trimester. There were 1 case of Trisomy 13 (IUFD at 32 wk), 1 case of Trisomy 18 (IUFD at 26+ wk), 1 case of Trisomy 21 (died at 1 day of age), all confirmed by cytogenetic studies. In both Trisomy 13 and Trisomy 18 cases, mothers were sickle cell traits. The 4 tumor cases were of children aged 2 to 15 yo with nasopharyngeal carcinoma (15 yo), neuroblastoma (3 yo), rhabdoid tumor arising from the prostate (8 yo), or primitive neuroectodermal tumor (2 yo), respectively. Only 7% of all deaths, or 4% of IUFD, were signed out as unknown etiology.

Conclusions: Determining causes of pediatric deaths can be challenging. A thorough autopsy can usually identify the etiology and additional diagnosis, which will serve as better guidance and consultation for the subsequent pregnancies. Text mining provides an effective tool to analyze free text reports for trend and new insights. A well structured report template helps to yield high quality text mining results.

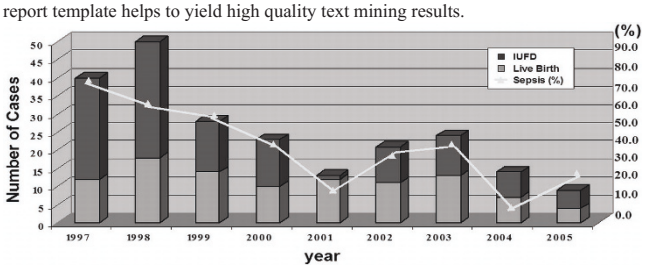

Table 1. Common etiology and frequency found in pediatric autopsies.

Etiology	All Deaths (n=228)		IUFD (n=125)	
	Cases	%	Cases	%
Sepsis	106	46.49	65	52.00
Congenital Disease	45	19.74	18	14.40
Twin Pregnancy	24	10.53	8	6.40
Pulmonary Hypoplasia	10	4.39	0	0.00
Tumor	4	1.75	0	0.00
Uteroplacental Insufficiency	25	10.96	21	16.80
Abruptio Placenta	15	6.58	12	9.60
Cervical Incompetence	2	0.88	0	0.00
Maternal Diabetes	18	7.89	9	7.20
Maternal Obesity	25	10.96	18	14.40
Maternal Sickle Cell Trait	12	5.26	9	7.20
Pre-eclampsia	8	3.51	6	4.80
Antiphospholipid Antibody Syndrome	1	0.44	1	0.80
Unknown	7	3.07	4	3.20

Bone & Soft Tissue

25 Comparative Gene Expression Profiling of Chordoma and Chondrosarcoma

NP Agaram, JH Schwab, PJ Boland, ND Socci, T Guo, S Doty, S Ferrone, JH Healey, CR Antonescu. Memorial Sloan-Kettering Cancer Center, New York, NY; Roswell Park Cancer Institute, Buffalo, NY; Sloan-Kettering Institute, New York, NY; The Hospital for Special Surgery, New York, NY.

Background: Chordoma and chondrosarcoma are malignant bone tumors characterized by their production of abundant extracellular matrix. These two tumor types are similar in their resistance to conventional therapeutic modalities, including radiation and systemic chemotherapy. Our goal was to delineate the gene expression profile of chondrosarcoma and chordoma tumors, in order to identify potential molecular therapeutic targets.

Design: A HG-U133A Affymetrix Chip platform was used to determine the variability of gene expression in 6 conventional chordomas and 14 conventional chondrosarcomas, which was compared to a control group of 45 soft tissue sarcomas. Statistical analyses were performed to identify discriminatory gene lists and Venn diagram was used to select non-overlapping, differentially expressed genes among gene lists. Validation of selected genes was performed by qPCR and immunohistochemistry on an extended subset of chondrosarcoma and chordoma tumors.

Results: By unsupervised hierarchical clustering, chordomas and chondrosarcomas grouped together in a genomic cluster distinct from a broad set of soft tissue sarcomas. They shared overexpression of many extracellular matrix genes including: *aggrecan, type II & type X collagen, fibronectin, connective tissue growth factor, fibromodulin, matrillin 3, chondroitin sulfate proteoglycan 4 (CSPG4), MMP-9, and MMP-19*. In contrast, *T Brachyury* and *CD24* are distinctly expressed in chordomas, as are *Keratins' 8,13,15,18 and 19*. Chondrosarcomas are distinguished by the high expression of *type IX* and *XI collagen*. Among these genes, *CSPG4* stands out as a promising therapeutic target, having already been extensively used as an immunotherapy target in patients with melanoma. Immunohistochemical analysis with CSPG4 mAb revealed positive staining in 48% and 62% of the chondrosarcoma and chordoma tumors, respectively.

Conclusions: Chordomas and chondrosarcomas share a similar gene expression profile, based on the overexpression of a significant number of extracellular matrix genes. *CSPG4* is one among numerous potential candidate genes, which can be further exploited for targeted therapy.

26 Is GLUT-1 a Specific Marker of Perineurial Differentiation? An Evaluation of GLUT-1 Expression in 82 Mesenchymal Tumors

WA Ahrens, BL Caron, AL Folpe. Mayo Clinic, Rochester, MN.

Background: GLUT-1, an erythrocyte-type glucose transporter protein expressed in juvenile hemangiomas, has recently been shown to be a sensitive marker of perineurial cells and their tumors, in a small number of cases. GLUT-1 expression has not, however, been systematically examined in other mesenchymal neoplasms. Importantly, GLUT-1 is known to play a critical role in the cellular response to hypoxia, as a downstream target of HIF1-alpha. Prompted by a recent report of GLUT-1 expression in epithelioid sarcoma, a tumor not generally felt to show perineurial differentiation, we examined GLUT-1 expression in a wide variety of mesenchymal tumors, specifically including tumors with spontaneous and/or therapy-related necrosis.

Design: 82 mesenchymal neoplasms (1 ASPS, 1 clear cell sarcoma, 3 endometrial stromal sarcomas, 5 epithelioid sarcomas, 4 ES/PNET, 2 fibromas, 3 FS, 6 GIST, 11 "MFH", 3 LMS, 9 lipomas, 3 dedifferentiated LPS, 2 MPNST, 2 myxoFS, 11 neurofibromas, 11 schwannomas and 5 synovial sarcomas were immunostained for GLUT-1, using a commercially available polyclonal antibody. Membranous staining in >5% of cells was scored as "positive".

Results: Normal perineurial cells were always GLUT-1 positive. All benign nerve sheath tumors showed a peripheral rim of positive perineurial cells, with 3 neurofibromas and 1 schwannomas showing more extensive staining. GLUT-1 expression was seen in 3 of 5 epithelioid sarcomas and the glands of one biphasic synovial sarcoma. Among untreated sarcomas, strong GLUT-1 expression was seen immediately adjacent to foci of coagulative necrosis in one endometrial stromal sarcoma, one FS and one dedifferentiated LPS. Diffuse GLUT-1 expression was seen in two "MFH" which had undergone neoadjuvant chemo/radiotherapy.

Conclusions: GLUT-1 is a highly sensitive marker of perineurial cells. In the absence of intratumoral necrosis, GLUT-1 expression appears to be relatively specific for perineurial cells and tumors, with "aberrant" immunoreactivity noted only in the glandular component of a single synovial sarcoma and in the majority of epithelioid sarcomas. GLUT-1 expression may reflect perineurial differentiation in epithelioid sarcoma; alternatively, it may reflect upregulation of this protein within hypoxic zones, given the propensity of this tumor to undergo spontaneous necrosis. In sarcomas exhibiting spontaneous or treatment-related necrosis, GLUT-1 expression likely represents a HIF1 mediated response to hypoxia, as described in epithelial tumors, and should not be taken as evidence of perineurial differentiation.

27 Detection of B-Catenin Gene Mutations in Paraffin-Embedded Sporadic Desmoid-Type Fibromatosis by Mutation-Specific Restriction Enzyme Digestion (MSRED): An Ancillary Diagnostic Tool

MFC Amary, B Idowu, L Islam, K Bousdras, P Pauwels, E Meulemans, TC Diss, AM Flanagan. Institute of Orthopaedics, UCL, Middlx, United Kingdom; Santa Casa School of Medical Sciences, Sao Paulo, Brazil; Royal National Orthopaedic Hospital, London; University College Hospital, London, United Kingdom; University Hospital, Maastricht, Netherlands; Universitair Ziekenhuis, Gent, Belgium.

Background: Desmoid-type fibromatosis is a locally aggressive deep soft tissue tumour with a high recurrence rate. Some cases are associated with familial adenomatous polyposis (FAP) and inherited mutations of the APC gene. Point mutations of the β-catenin gene have been identified in sporadic fibromatosis. These produce amino acid substitutions, stabilising β-catenin, which binds transcription factors and switches on the Wnt signaling pathway. Distinguishing between desmoid-type fibromatosis and other spindle cell lesions can be difficult particularly in needle cores. The aim of this study was to determine the value of MSRED in the diagnosis of fibromatosis.

Design: 69 cases were diagnosed morphologically as desmoid-type fibromatosis, 16 as superficial fibromatosis, 5 as solitary fibrous tumour, 4 as nodular fasciitis and 1 as periosteal fasciitis. These 95 cases were analyzed by MSRED. The PCR products were digested by restriction enzymes (table 1). A restriction site was present for analysis of the common mutation in codon 41. Mismatch primers were designed for two mutations in codon 45.

Results: Mutations were present in 60 cases (87%) diagnosed as desmoid-type fibromatosis, 3 located in the abdominal wall, 4 involving the foot and 53 in soft tissue elsewhere. Of these, 31 (52%) were in codon 45 (TCT>TTT), 24 (40%) in codon 41 (ACC>GCC) and 5 (8%) in codon 45 (TCT>CCT). No mutations were detected in the other lesions studied.

Conclusions: This is the largest study to date of molecular analysis of β-catenin mutations in paraffin-embedded material. Diagnosing fibromatosis can be difficult, especially in needle core samples and exploiting these mutations in this manner can complement light microscopy in reaching a diagnosis.

Restriction enzymes and the expected product sizes for detection of β-catenin exon 3 mutations

Codon	Nucleotide substitution	Amino acid substitution	Product size (bp)	Restriction endonuclease (RE)	RE Product size (bp)
41	ACC - GCC	T41A	120	TspRI	WT 120, Mutant 88+32
45	TCT - TTT	S45F	141	DdeI	WT 117+24, Mutant 141
45	TCT - CCT	S45P	101	BseRI	WT 101, Mutant 89+12

28 Analysis of 134 Formalin-Fixed Paraffin-Embedded Synovial Sarcomas by Conventional RT-PCR, Real Time RT-PCR and Dual Colour FISH

MFC Amary, F Berisha, FDC Bernardi, JS Reis-Filho, TC Diss, AM Flanagan. Institute of Orthopaedics, UCL, London, United Kingdom; Santa Casa School of Medical Sciences, Sao Paulo, Brazil; Royal National Orthopaedic Hospital, Middlx; University College Hospital, London; Breakthrough Breast Cancer Research Centre, London.

Background: Synovial Sarcoma (SS) is an aggressive neoplasm accounting for 5-10% of sarcomas, and although typically occurring in the extremities of young adults is also found in atypical sites and ages. SS consistently carries t(X;18) resulting in SYT-SSX1, SYT-SSX2 and rarely SYT-SSX4 fusion transcripts.

Design: 134 cases [103 monophasic(MP), 31 biphasic(BP)] were included in our study: in all cases SS was either the primary diagnosis or was considered high in the differential. Conventional and real-time RT-PCR, and FISH were used to confirm the diagnosis and to analyse the sensitivity of these tests in paraffin-embedded material. 113 of the cases, were placed in a tissue microarray (TMA) and analysed by dual colour FISH using a SYT breakapart probe: cases with a breakapart signal in at least 20% of the cells were scored positive.

Results: RNA of suitable quality was extracted in 131 cases: 126 (96%) showed SYT-SSX fusion (74 SYT-SSX1, 52 SYT-SSX2) using real-time RT-PCR and 121 using conventional RT-PCR. Of the 113 TMA cases, 12 (11%) could not be analysed due to core loss or weak/absent signals. Of the 101 remaining cases, 87 (86%) showed SYT rearrangement. 15 cases had multiple copies of the SYT gene and 4 cases, considered negative, showed loss of one signal (spectrum green). Of 3 cases not analysed by RT-PCR due to inadequate RNA, one was positive by FISH. SYT-SSX1 was present in 56 MP and 18 BP; SYT-SSX2 in 41 MP and 11 BP. Poorly differentiated areas were present in 44 cases (31%). 5 cases were negative by all methods, 127 were positive with at least one of the methods and 2 could not be analysed.

Conclusions: Combining molecular methods provide a powerful aid to diagnosing SS. RT-PCR showed higher sensitivity than FISH, though FISH has the advantage of direct visualisation of the tissue and in 1 case supported the diagnosis where poor RNA prevented analysis by RT-PCR. FISH can be difficult to interpret when there are multiple copies of the SYT gene or loss of one of the signals due to absence of the reciprocal translocation. There was no statistically significant difference between BP and MP in terms of fusion type. The 4 negative cases occurred at unusual sites and SS was not the primary diagnosis: these may represent different diseases.

29 Dissecting Osteosarcoma Genesis by Gene Expression Pathway Profiling

JK Anninga, IH Briaire-de Bruijn, S Romeo, J Oosting, RM Egeler, AHM Taminiau, PCW Hogendoorn, AM Cleton-Jansen. LUMC, Leiden, Netherlands.

Background: Osteosarcoma (OS) is the most prevalent primary malignant bone tumour of children and young adults. Chemotherapy treatment has improved prognosis but now has reached a plateau in terms of increasing survival and therefore knowledge of molecular mechanisms for new targets for therapy is needed. The putative cell of origin of OS is unknown however osteoblasts and their mesenchymal stem cell precursors (MSC) are the most likely.

Design: In order to identify signalling pathways differentially expressed in OS versus its presumed normal counterpart, genome wide expression profiles were generated from 25 high grade central OS pre-chemotherapy biopsies, 5 MSC populations and these same MSCs differentiated to osteoblasts (DO). Genes that were differentially expressed between OS, MSC and DO were analysed in the context of the pathways in which they function using the GenMAPP program. Especially pathways that were known to be involved in MSC differentiation were studied. Immunohistochemistry on tissue arrays was performed to verify expression at the protein level.

Results: Unsupervised hierarchical clustering could not distinguish OS with good prognosis from those with poor, nor good response to chemotherapy versus poor. MSCs, DOs and OSs clustered separately and thousands of differentially expressed genes could be distinguished. Components of the p53 pathway are down regulated in OS, both TP53 and two downstream genes p21/CDKN1A and PUMA/BBC3 are significantly lower in OS than in MSC and osteoblasts. Immunohistochemistry for p53 and p21 showed absence of p21, also in cases with positive p53, the latter probably compliant with mutated p53. Several upstream components of the Wnt signaling pathway are down regulated in OS, e.g. the ligand Wnt5a and the Frizzled receptors FZD6 and FZD7. Two genes involved in degradation of β-catenin protein, the key effectors of Wnt signaling, Axin and GSK3-β show decreased expression, suggesting that Wnt signaling is active, but no longer under control of the regular signals. Immunohistochemistry for β-catenin demonstrated nuclear localization in a subset of OS.

Conclusions: Comparison of expression profiles between OS and its progenitors MSC and DO revealed marked differences in signal transduction, especially signaling mediated by p53 and β-catenin. This will help in understanding the biology op OS in more detail.

30 Dedifferentiation in Gastrointestinal Stromal Tumor (GIST) to an Anaplastic KIT Negative Phenotype – A Diagnostic Pitfall

CR Antonescu, JL Hornick, GP Nielsen, M Mino-Kenudson, G Wong, C Corless, CDM Fletcher. Memorial Sloan-Kettering Cancer Center, New York, NY; Brigham & Women's Hospital, Boston, MA; Massachussetts General Hospital, Boston, MA; Oregon Science & Health University, Portland, OR.

Background: Most GISTs can be recognized by their uniform cytologic features and overexpression of KIT oncoprotein. Changing phenotype with complete loss of KIT reactivity has been previously described after chronic imatinib treatment, however this phenomenon has not been reported in imatinib-naïve tumors. We have identified 4 patients with abrupt transition from a classic KIT positive spindle cell GIST to an anaplastic KIT negative tumor, in which we sought to investigate the underlying molecular mechanisms of tumor progression.

Design: Histologic, immunohistochemical, and molecular analysis was performed on each of the two components. Genomic DNA PCR for *KIT* and *PDGFRA* hot spot mutations, as well as FISH for detecting *KIT/PDGFRA* gene copy number alterations were performed. *P53* mutational analysis was performed in 3 cases.

Results: There were 3 males and 1 female, with an age range of 23-55 years old. All tumors were located in the stomach. Only one patient had prior exposure to imatinib and all except one had metastatic implants present at diagnosis. The dedifferentiated component in all tumors had an anaplastic/pleomorphic phenotype, with tumor giant cells, high mitotic activity and necrosis. This component showed consistent loss of KIT and CD34 expression, while acquiring cytokeratin (3/4) or desmin (1/4) reactivity. Three patients had a wild-type genotype in both components, while 1 had a *KIT* exon 11 deletion in both components. FISH showed gene copy abnormalities in the dedifferentiated component in 3/4 cases tested, with loss of one KIT copy in 1 case and small level of KIT amplification in the other 2 cases, while a normal copy number was seen in the KIT positive areas. *P53* mutation was identified in 1/3 cases tested and was present in both components.

Conclusions: Dedifferentiation, defined as tumor progression from a conventional KIT positive GIST to an anaplastic/pleomorphic KIT negative tumor has not been previously well-characterized and can represent a diagnostic pitfall. This phenomenon can be seen either de-novo or after chronic imatinib exposure. The most common abnormality identified in the dedifferentiated component was genetic instability, either represented by loss of heterozygosity or small level amplifications of KIT.

31 *EWS-CREB1* Is the Predominant Gene Fusion in So-Called Angiomatoid Fibrous Histiocytoma (AFH)

CR Antonescu, P Dal Cin, K Nafa, LA Teot, CDM Fletcher, M Ladanyi. Memorial Sloan-Kettering Cancer Center, New York, NY; Brigham&Women's Hospital, Boston, MA; Children's Hospital of Pittsburgh, Pittsburgh, PA.

Background: AFH is a hemorrhagic, multicystic neoplasm, associated with distinctive histiocytoid morphology and frequent positivity for DES, CD68 and EMA, which occurs typically in the soft tissues of the limbs and trunk of children and adolescents. The molecular hallmark of AFH is not well defined, with 2 examples each reported to harbor either a *FUS-ATF1* or *EWS-ATF1* fusion, although large confirmatory series of these results are lacking. In this study, we investigated the gene fusions in a group of 8 AFHs identified in our files with otherwise typical histologic features and immunoprofiles.
Design: All cases were subjected to RT-PCR for *EWS-ATF1* and *EWS-CREB1* fusion. FISH for both *EWS* and *FUS* gene rearrangements was performed in 6 cases.
Results: There were 5 males and 3 females with a mean age at diagnosis of 26 years (3-79). The tumors were located in the trunk, 4, limbs, 3, and head and neck, 1. All tumors were positive for desmin and 7/8 also for CD68. In addition 4/4 tumors tested expressed CD99. By RT-PCR, 7/8 tumors showed the presence of *EWS-CREB1* fusion, while 1 tumor had an *EWS-ATF1* transcript. FISH showed evidence of *EWS* rearrangement in 6/6 cases tested, while it did not show the *FUS* gene to be altered in any case. Karyotypic analysis had been performed in one tumor and it showed the presence of a t(2;22)(q33;q12), as expected with *EWS-CREB1* fusion.
Conclusions: We report for the first time the presence of *EWS-CREB1* in AFH, which appears to be the most frequent gene fusion event in this tumor (7/8 cases tested). *EWS-CREB1* is a novel translocation recently described by our group in clear cell sarcoma of the GI tract. *EWS-ATF1*, identified in one of our AFH cases and two others in the literature, is the most common genetic abnormality seen in soft tissue clear cell sarcoma. Thus, identical or highly related fusions involving *ATF1* and *CREB1* are found in two distinct sarcoma types, and we speculate that these fusions may be able to induce different differentiation programs in mesenchymal precursor cells, unlike most other sarcoma gene fusions.

32 Juxtacortical Chondromyxoid Fibroma of Bone: A Unique Variant. A Study of 19 Cases

AC Baker, L Rezeanu, S O'Laughlin, KK Unni, MJ Klein, GP Siegal. University of Alabama at Birmingham, Birmingham, AL; Mayo College School of Medicine, Rochester, MN; Mt. Sinai, New York, NY.

Background: Chondromyxoid fibroma (CMF) of bone is a rare neoplasm of the appendicular skeleton occurring in young adults as an eccentric, intramedullary lesion in the metaphyseal region of the long bones. We report 19 cases of a poorly recognized subtype of this neoplasm, which arises on the surface of long bones. This lesion erodes the cortical surface causing a periosteal reaction and often extends into the soft tissues. Therefore, this entity needs to be included in the differential diagnosis of bone surface lesions since it may be mistaken for a biologically more aggressive neoplasm.
Design: A 47 year Mayo Clinic retrospective review identified 259 CMF cases, 14 of which were parosteal. Two additional cases were diagnosed at the University of Alabama at Birmingham over a 16 year period and another 3 cases were from one of our authors' files. Most of the cases were seen in consultation. We reviewed the radiographic and pathologic findings of all 19 cases.
Results: Juxtacortical CMF occurred over a large age range (12-82 years of age). The median age was 40.2 years and there was a slight male predilection (5:4). The most common clinical presentation was bone pain. All of the lesions were solitary, radiolucent surface lesions with sclerotic margins that did not involve the medullary canal, but extended focally into the overlying soft tissues. The majority of the lesions were located in the metaphysis of the proximal tibia. Histologically, the tumors had all the characteristic features of CMF, which consisted of a lobular proliferation of spindle to stellate cells in a myxoid stroma with peripheral hypercellularity, mixed with chondroid foci and fibrous tissue. Additionally, several of the lesions contained distinctive areas of calcification, which is not a regular feature of conventional CMF. Where follow-up was available (12 cases), 11 cases were noted to be cured with simple excision.
Conclusions: When confronted with a lesion on the surface of bone, CMF should be included in the differential diagnosis. The pathologist must be aware of the clinical presentation and radiologic findings to ensure the correct diagnosis is made. Fortunately, the morphology of this benign lesion is similar to conventional CMF with the exception of occasional foci of calcification. Conservative therapy, consisting of complete excision, is the treatment of choice with few, if any, sequelae.

33 High Grade Surface Osteosarcoma (HGSOS). The Rizzoli Institute Experience

F Bertoni, C Inwards, E Staals, P Bacchini. Istituto Ortopedico Rizzoli, Bologna, Italy; Mayo Clinic, Rochester, MN.

Background: HGSOS represents a rare subtype of osteosarcoma that arises on the surface of bone. It accounts for less than 10% of surface osteosarcomas in our files at the Rizzoli Institute.
Design: Criteria for inclusion in the study included: 1) Surface based tumor confirmed by radiographic and/or gross and histologic features. 2) histologic features of a high grade (Broders grade 3 and 4) osteosarcoma (ogs). 26 tumors fulfilled these criteria. Histologic sections and gross specimens were available in all cases. Radiographs were available in 23 cases.
Results: There were 7 women and 19 men aged 9-66 yrs (mean 24 yrs; median 21 yrs). All of the tumors involved the surface of a long bone in the leg. 20 tumors were in the diaphysis (femur: 11, tibia: 7, and fibula: 2). 4 pts had lesions in the distal femur and 2 pts in the proximal tibia. Radiographically, the majority of the lesions (19/23) showed dense to moderate mineralization. Circumferential involvement (varying from 20 to 100%) of the host bone was seen in 20/23 (87%) of the pts. Minimal medullary involvement was seen in 9 tumors, and up to 20% was present in 5 tumors. Histologically, 21were gr 4 osteoblastic ogs, and 5 were gr 4 chondroblastic ogs. Lung metastases were detected histologically in 4 pts and bone metastases in one pt. Treatment: (25 pts): 21 had surgery and chemotherapy (13 neoadjuvant, 8 adjuvant). 19 of these 21 pts had a wide margin. One each in the neoadjuvant and adjuvant group had a marginal margin. 3 pts had only surgery with a wide margin and one who presented with metastases was treated only with chemotherapy. Follow-up: (25 pts) Follow-up time ranged from 1 to 780 mos: average 111 mos; median 73 mos). All of the 13 pts treated with surgery and neoadjuvant chemotherapy are alive; 11 have no evidence of disease (NED) and 2 have NED following surgery for lung metastases. Of the 8 pts treated with surgery and adjuvant chemotherapy, 6 are alive (one with bone metastases) and 2 dead of disease.
Conclusions: HGSOS is the rarest subtype of surface osteosarcoma. It has similar clinicopathologic features and prognosis as conventional central osteosarcoma. There is a predilection for diaphyseal involvement of the long bones. In this series, pts treated with surgery and neoadjuvant chemotherapy achieved better results than those treated with surgery and adjuvant chemotherapy.

34 Expression of Insulin-Like Growth Factor 2 in Synovial Sarcoma

D Borys, JB Taxy, R Garcia, H Yee, L Chiriboga, J Wei, MA Greco. NYU School of Medicine, New York, NY; University of Chicago, Chicago, IL.

Background: Synovial sarcomas are aggressive soft tissue neoplasms often characterized by monophasic and biphasic spindle and epithelioid cell morphology. Despite advances in the therapy of local disease, distant metastasis remains the predominant cause of death. Accordingly, there is a need for alternate prognostic and therapeutic markers. Insulin-like Growth Factor 2 is critical both for tumor formation in vivo as well as for protection against apoptosis in vitro. The present study was done to determinate the frequency of expression of IGF 2 in synovial sarcoma.
Design: A tissue micro array was created using paraffin embedded samples from 16 synovial sarcoma cases from the archival surgical pathology files.The age of the patients ranged from 12 to 55 (mean 38). 10 patients had monophasic and 6 biphasic synovial sarcomas. 5 patients had pulmonary metastasis; 1 had a local recurrence in the primary site. Immunohistochemistry was done with polyclonal rabbit antibody (Cat. SC-5622 Santa Cruz, CA).A scoring system was based on expression of IGF2 as 1+ < 25%, 2+ < 50%, 3+ > 50%.
Results: In 13/16 (81%) synovial sarcoma cases IGF2 immunoreactivity was detected as strong cytoplasmic pattern. In biphasic synovial sarcoma IGF2 was strongly (3+) expressed in the epithelial component, and weaker (1+) in the spindle cell component. In monophasic synovial sarcoma IGF2 was strogly expressed in spindle cell component (3+). 5 / 5 patients with pulmonary metastasis, and 1/1 patient with local recurrence had strong (3+) IGF2 cytoplasmic expression.
Conclusions: Strong expression of IGF2 was present in the majority of our cases , and all cases with metastatic and recurrent disease, suggesting the importance of this oncoprotein in the tumorogenesis of synovial sarcoma. Targeting the IGF2 signaling pathway may represent another therapeutic modality for treating synovial sarcoma.

35 Prognostic Value of Myogenic Differentiation in Adult Soft Tissue Sarcomas (STS). A Study of 460 Cases from the French Sarcoma Group (FSG)

JM Coindre, C Dupin, M Bui, MC Chateau, F Collin, L Guillou, A Leroux, B Marques, JJ Michels, D Ranchere, YM Robin, P Terrier, M Trassard, I Valo. Institut Bergonié, Bordeaux, France; French Sarcoma Group, France.

Background: Most adult STS with no specific genetic alterations are represented by leiomyosarcomas (LMS), adult rhabdomyosarcomas (RMS), pleomorphic liposarcomas (LPS), myxofibrosarcomas (MFS) and poorly-differentiated sarcomas or so-called malignant fibrous histiocytomas (MFH). This category of sarcomas is often difficult to histotype but a myogenic differentiation has been reported to be more aggressive.
Design: 482 cases of adult STS initially diagnosed as LMS (187), adult RMS (15), pleomorphic LPS (25), MFS (42) and MFH (213) were retrieved from the FSG database. They were re-classified after histological review (482) and immunohistochemistry for muscular markers (431). The following parameters were studied: age, sex, tumor location (internal trunk versus other locations), size, depth, grade and myogenic differentiation (LMS and adult RMS versus MFH, MFS and pleomorphic LPS). We performed univariate and multivariate analyses for metastasis-free survival.
Results: After re-classification, 22 cases were ruled out (16 dedifferentiated LPS and 6 other sarcomas). The remaining 460 cases were classified as LMS (211), adult RMS (19), pleomorphic LPS (24), MFS (71) and MFH (135). Median age was 62 years (23 to 98). Tumor location was members (327), internal trunk (49), trunk wall (71) and head and neck (13). Median size was 9 cm (1 to 35) and 389 cases were deeply-located. Median follow-up was 68 months and 169 patients experienced distant metastasis. Univariate analysis indicated that internal trunk location ($p=6.7x10^{-5}$), size (p=.001), depth ($p=8x10^{-5}$and myogenic differentiation ($p=8.7x10^{-5}$) were significant predictor of metastasis. Multivariate analysis retained tumor depth, myogenic differentiation and internal trunk location for predicting metastasis.
Conclusions: This study showed that myogenic differentiation is an adverse prognostic factor among spindle cell and pleomorphic adult STS with no specific genetic alterations. These tumors are difficult to histotype with still a set of poorly-differentiated sarcomas/MFH.

36 CD10 Expression in Epithelioid Hemangioendothelioma: A Preliminary Study

K Cunningham, D Howarth, B Perez-Ordonez, D Hwang, I Weinreb. University Health Network, Toronto, ON, Canada; Mount Sinai Hospital, Toronto, ON, Canada.

Background: Epithelioid hemangioendothelioma (EHE) is a rare vascular neoplasm of intermediate malignant potential. It is characterized by epithelioid cells that form occasional intracytoplasmic lumina and are often embedded in a myxoid stroma. This tumor has been described at various soft tissue and visceral sites and may be difficult to distinguish from primary or metastatic carcinomas, especially in biopsies. In addition, EHE can stain with keratins and lack one or more of the traditional vascular markers, making this diagnosis more difficult. CD10 is an activation marker that stains a variety of tissues including endometrial stroma, myoepithelial cells, hepatic canaliculi and renal cell carcinomas. The aim of this study was to examine the expression of CD10 in EHE, which has not been done previously.

Design: Nine cases of primary EHE were retrieved from our archives and stained with immunohistochemical antibodies to various keratins, vimentin, factor VIII, CD31, CD34 and CD10. The age range of the patients was 24-74 years old and there were 5 male and 4 female patients. The tumors included three cases arising in the liver, two in the lung/pleura, two in skin, one in the sternocleidomastoid muscle and one in the anterior mediastinum/thymus. Two cases showed metastases to the skin, which were also stained with the above markers.

Results: The tumors showed typical histology for EHE with one case showing a transition to a higher grade tumor. All nine lesions were positive for at least one of the vascular markers. Two cases were positive for CK 7, but no other epithelial markers. Six of the nine primary tumors stained strongly and diffusely with CD10 in a cytoplasmic staining pattern, and highlighted the intracytoplasmic vascular lumina. One additional case stained focally. CD10 did not stain endothelial cells in normal vessels. The two cases that had metastatsized to the skin also showed positive staining however, the primary skin EHE's did not stain for CD10.

Conclusions: CD10 appears to be a sensitive, but not specific marker for EHE. This may serve useful in difficult cases that may show weak staining for vascular markers, particularely when used as part of a panel to assess candidate lesions. The negative staining in primary skin EHE and positive staining in metastases to the skin, may serve to differentiate these lesions, although more cases should be studied to examine this issue further.

37 Osterix, Sox9, Master Transcription Factors on Tissue Microarrays in the Osteoid Osteoma, Osteoblastoma, Chondromyxoid Fibroma and Chondroblastoma

J Dancer, A Ayala, B Czerniak. The Methodist Hospital, Houston, TX; M.D. Anderson Cancer Center, Houston, TX.

Background: Osterix is a recently identified zinc finger–containing transcription factor and plays an essential role in osteoblast differentiation at an early stage following Runx2-dependent mesenchymal condensation. Sox9 encodes a HMG-box transcription factor that has been implicated in a master regulator of the differentiation of mesenchymal cells into chondrocytes.

Design: We evaluated the expression of Osterix and Sox9 in four types of rare benign bone tumors including 12 osteoid osteoma, 12 osteoblastomas,8 chondromyxoid fibromas and 8chondroblastomas in order to better understand the molecular pathogenesis of benign bone tumors. A tissue microarray(TMA) was constructed with these four types of bone tumors. The cases are represented by one to three 1mm cores for a total of 112 cores on array. A section of mouse embryo was used for the internal control of TMA. Immunohistochemistry for Osterix (provided by Molecular Genetics) and Sox9 (Chemicon) were performed. Staining was interpreted as strongly or weakly positive, nuclear or cytoplasmic positive, negative or uninter pretable.

Results: Immunohistochemical expression profiles for four benign bone tumors are presented in the below table.

Expression of Osterix and Sox9

	OsterixI	Sox9
OO	12/12 (100%)	0 /12 (0%)
OB	12/12 (100%)	6/12 (50%)
CMF	1/8 (12%)	7/8 (88%)
CB	3/8 (37%)	8/8 (100%)

OO; Osteoid Osteoma, OB;Osteoblastom, CMF; Chondromyxoid fibroma, CB;Chondroblastoma

Osteoid osteoma and osteoblastoma showed 100% strong nuclear expression of Osterix. Whereas, weak cytoplasmic expression of Osterix was observed in one chondromyxoid fibroma. Three chondroblastoma showed positive nuclear expression of Osterix. Strong nuclear expression of Sox9 was detected in all 8 chondroblastoma. Five osteoblastoma showed diffuse nuclear Sox9 staining. Focal nuclear Sox9 expression was demonstrated in one osteoblastoma.

Conclusions: These findings confirm that osteoblastoma and osteoid osteoma have phenotypic features corresponding to the early condensational phase of osteogenic differentiation. In contrast, chondroblastoma and CMF have phenotypic features corresponding to the early condensational phase of cartilaginous differentiation. A subset of osteoblastoma and chondroblastoma appear to have biphasic phenotypic features of both osteogenic and cartilaginous differentiation.

38 Loss of CXCR4 Nuclear Immunoreactivity in Synovial Sarcoma Correlates with Poor Survival

AP Dei Tos, S Grisanti, E Rossi, L Ardighieri, VD Ferrari, V Amoroso, L Bercich, G Marini, S Rossi, F Facchetti, F Facchetti. Spedali Civili, Brescia, Italy; University of Brescia School of Medicine, Brescia, Italy; Regional Hospital, Treviso, Italy.

Background: CXCR4, the receptor for the chemokine SDF-1, is overexpressed in many human tumors. CXCR4 activation has been described in osteosarcoma, rhabdomyosarcoma and Ewing's sarcoma both in vivo and in vitro, but its role in synovial sarcoma (SS) has not been elucidated so far. Gene products of the HER oncogenic family, such as EGFR and HER2, have been described to be overexpressed in patients with SS and proposed as potential therapeutic targets. As CXCR4 and HER2 are known to be functionally linked in breast cancer cell lines, we analyzed CXCR4, HER2 and EGFR expression in a SS.

Design: Fifteen SS patients were included in the study. In all cases morphological diagnoses were confirmed molecularly by FISH or RT-PCR. HER2 and EGFR expression were determined immunohistochemically while HER2 gene status was assessed by FISH analysis. CXCR4 expression was determined with an anti-human CXCR4 monoclonal antibody (Clone 44716, R&D Systems, Minneapolis, USA). CXCR4 nuclear expression was correlated with outcome.

Results: All patients were classified high-risk (stage III-IV) according to the AJCC/UICC VI Edition Staging System for soft tissue sarcomas. In all samples IHC analysis for HER2 was negative and no amplification was found by FISH. EGFR expression was observed in 13/15 patients. CXCR4 immunoreactivity was identified in 9/15 cases. CXCR4 and EGFR were coexpressed in 8/15 tumors. Follow-up ranged from 9 to 120 months. After a median follow-up of 37 months, 7 patients were dead of SS, 8 patients were alive (7 of them are disease-free and one relapsed to the lung). All alive and disease-free patients showed nuclear CXCR4 expression whereas 6/7 dead patients lacked nuclear CXCR4 expression. (p = 0,0008)

Conclusions: 1. Loss of nuclear CXCR4 expression is associated with fatal course and may represent a novel prognostic factor. **2.** CXCR4 is frequently coexpressed with EGFR but not with HER2.**3.** In contrast with previous reports HER2 seems not be involved in the carcinogenesis of SS.

39 Gnathic Well Differentiated Osteosarcomas: A Clinicopathologic Study of 9 Cases

V Deshpande, GP Nielsen, AE Rosenberg. Massachusetts General Hospital, Boston, MA.

Background: Osteosarcoma (OS) of craniofacial bones accounts for 6 to 10% of all cases. The mandible and maxilla are most frequently affected, accounting for 50% and 25% of cases respectively. Typically gnathic OSs are high grade and demonstrate a chondroblastic phenotype. Well differentiated intramedullary OSs and surface OSs have only rarely been described in this anatomical site. Well differentiated OSs cause diagnostic difficulties because of thier overlapping features with other fibroosseous lesions of the head and neck. Herein we describe the clinicopathologic features of 9 cases of gnathic well differentiated OS.

Design: The surgical pathology and consultation files of James Homer Wright Laboratories and one of the authors were reviewed to identify well differentiated OSs of the jaw bones. Clinical data was retrieved from the patient's medical record. HE-stained sections were examined in all cases.

Results: Nine cases of well differentiated OS- 5 maxillary and 4 mandibular, were identified. The mean age was 43 years (range 20 to 66). Five patients were males and 3 females. Imaging showed an intramedullary lytic and sclerotic lesion in three cases, and a sclerotic surface lesion in one case. Treatment consisted of wide local excision in 8 cases. Grossly one of the lesions was a mandibular exophytic bony mass, while the other tumors were predominantly intramedullary. Tumor size varied from 0.5 to 6 cm (mean 1.9). All 9 tumors contained well developed osseous trabeculae surrounded by sparsely to moderately cellular fibroblastic tumor cells. The nuclei were monomorphic, vesicular with small nucleoli and showed only rare (<1/10HPF) mitotic figures. Chondroblastic differentiation was noted on the surface of two lesions. Dedifferentiated elements were not present. Follow-up information was available on five cases (mean 15 months) and no local recurrence or metastasis was reported during this period.

Conclusions: Well differentiated OSs involve gnathic bones and morphologically resemble appendicular surface (parosteal) and intramedullary well differentiated OSs. Wide local excision appears to be the treatment of choice. Additional follow-up will help further define the biological behavior of this apparently indolent neoplasm.

40 Epithelioid Hemangioendothelioma of Soft Tissue: An Outcome Study of 46 Cases with a Proposal for Risk Stratification

AT Deyrup, SW Weiss. Emory University, Atlanta, GA.

Background: Epithelioid hemangioendothelioma (EHE) of soft tissue is a distinctive vascular tumor that has been variously considered a tumor of borderline malignancy and low grade angiosarcoma. The majority of cases are associated with low mortality, but some metastasize and occasionally result in death. We analyzed our experience to determine if a method for stratifying risk for mortality could be developed.

Design: Forty-six EHE referred in consultation and accessioned between 1990 and 2004 were retrieved. Tumors were evaluated with respect to location, size, cytologic atypia (low vs high), mitotic activity per 10 high power fields and the presence of tumor cell spindling and necrosis. Follow-up information was obtained for all cases. For actuarial analysis, disease-specific overall survival was evaluated using univariate and multivariable analysis.

Results: Most tumors occurred in adults (range 9-93 yrs) and affected women predominantly (27F:19M). They developed in the head and neck (7), extremities (27), mediastinum (4), trunk (5), and genitals (2) and retroperitoneum (1). and ranged in size from (0.5 - 18 cm). Clinical follow-up was obtained for all patients and ranged from 1.5 to170 months (mean 57.9 months); 31 patients were alive without disease, 2 patients were alive with disease, 6 patients died of disease, 5 died of other causes and 1 died of unknown cause. Metastasis developed in 11/46 patients and involved lungs (6), lymph nodes (5), liver (3) and bone, soft tissue and the retroperitoneum (1 each). Treatment modality was known for 40 patients: 23 were treated surgically, 14 were treated with surgery and chemotherapy and/or radiation therapy, 2 were treated palliatively and 1 received only radiation therapy. By univariate analysis, mitotic activity and size were associated with higher mortality (p=0.0008 and p=0.027, respectively). By multivariable analysis, increasing mitotic activity (p=0.0016, hazard ratio 2.63)

and size (p=0.045, hazard ratio 1.24) were associated with decreased survival. Those tumors with mitotic activity >=1/10 high power fields and size >= 3.5 cm had the worst prognosis (p=0.0013). Tumor site, cytologic atypia, the presence of necrosis and tumor spindling were not significant.

Conclusions: Patients with soft tissue EHE can be stratified into low and high risk groups for mortality based on a combination of size and mitotic activity. By differentiating between these two groups, it will be possible to better refine therapeutic options.

41 p63 Is Expressed in Giant Cell Tumors of Bone

B Dickson, B Eslami, J Wunder, P Ferguson, R Kandel. Mount Sinai Hospital, Toronto, ON, Canada; Harvard School of Dental Medicine, Boston, MA; Mount Sinai Hospital, University of Toronto, Toronto, ON, Canada.

Background: Diagnosis of the different types of giant cell-rich tumors of bone and soft tissue can be difficult to differentiate when there is limited sampling such as in needle core biopsies. Previously we observed that giant cell tumors of bone can express p63 and cyclin D1, cell cycle regulators. The purpose of this study was to determine if p63 expression was specific to giant cell tumors of bone and soft tissue and whether it could be used to aid in the diagnosis of these tumors.

Design: Cases of giant cell tumour (GCT) of bone (n=16), GCT of soft tissue (GCT-ST, n=5), central giant cell granuloma (CGCG, n=12), GCT of tendon sheath (GCT-TS, n=13), pigmented villonodular synovitis (PVNS, n=9), aneurysmal bone cyst (ABC, n=7), and osteosarcoma (OS, n=10) were retrieved from the archives as approved by institutional review. Histological sections of paraffin embedded tissue were reviewed by light microscopy to confirm the diagnosis. Sections from each case were stained for p63 or cyclin D1 using standard immunohistochemical methods.

Results: All cases of GCT of bone expressed p63 in mononuclear cells. Less than 20% of cells were immunopositive and they were distributed diffusely throughout the tumor. Very rare multinucleated cells had some weakly positive nuclei. Only 2/7 (29%) cases of ABC expressed p63. No p63 immunoreactivity was detected in any of the CGCG or the soft tissue variant of GCT. Other giant cell-containing soft tissue tumors such as PVNS and GCT of tendon sheath were negative. Ten cases of OS were also negative. In contrast differential expression of cyclin D1 in tumors was not observed as it was detected in most cases of GCT of bone and soft tissue and GCCG as well as in GCT-TS (85%), PVNS (44%), OS (36%) and ABC (33%). Both mononuclear and multinucleated cells were positive.

Conclusions: p63 expression is expressed predominantly in giant cell tumors of bone and may be suitable to use as a marker to differentiate this tumor from the other types of giant cell-containing bone and soft tissue tumors examined in this study. It is not clear why some ABCs express p63. It may be that they are related in some way to GCT. Interestingly, the absence of p63 expression in CGCG and GCT of soft tissue suggest that these tumors may have a different pathogenesis than GCT of bone.

42 Tyrosine Kinase Signaling in Fibromatosis

JH Fasig, BW Whited, WD Dupont, SJ Olson, JM Cates. Vanderbilt University Medical Center, Nashville, TN.

Background: Deep fibromatoses are locally aggressive tumors that cause significant morbidity. Despite reports of c-kit, PDGFR, and COX-2 expression in some cases, therapeutic benefit of kinase inhibitor and NSAID therapy is unpredictable. Variability in the expression level or functional activity of target molecules may be responsible for this phenomenon. A better understanding of growth regulatory signaling pathways in fibromatosis is necessary to determine the theoretical potential of inhibitor therapy.

Design: 27 cases of deep fibromatosis involving soft tissues of the extremities or trunk were retrieved from the surgical pathology files at VUMC; intra-abdominal cases were excluded. Five cases of superficial fibromatosis were studied for comparison. A tissue microarray (TMA) was constructed and studied by IHC for expression of focal adhesion kinase (FAK), c-met, platelet-derived growth factor receptor-β (PDGFRβ), epidermal growth factor receptor (EGFR), Her2, and c-kit. Receptor tyrosine kinase (RTK) mediated signaling activity was analyzed by IHC for the phosphorylated isoforms of EGFR, p44/42 mitogen-activated protein kinase (MAPK), STAT3, and Akt. Since most lesional cells stained uniformly within each TMA core, only staining intensity was scored (using a four-tiered scale). Results were correlated with total tumor volume using one-way ANOVA and disease-free survival by the log rank test.

Results: IHC results are presented in the table below. No staining for HER2 or c-kit was observed in any of the cases. None of the markers studied correlated with either tumor volume or disease-free survival. Similar patterns of IHC staining were observed in both deep and superficial variants of fibromatosis.

Conclusions: RTK activity is detectable in most cases of deep fibromatosis, and does not appear to be mediated by EGFR, HER2, or c-kit. In contrast, PDGFRβ is expressed at high levels in these tumors. Alternative mechanisms for MAPK, Akt, and STAT3 activation include signaling through the c-met and FAK pathways. Several of these signaling proteins can now be targeted by specific molecular therapeutic agents. This provides a theoretical rationale for novel treatment modalities for patients with desmoid tumors.

Signaling protein expression in deep fibromatosis

IHC Marker	0	1+	2+	3+
PDGFRβ	0%	0%	22%	78%
FAK	0%	38%	63%	0%
c-met	11%	44%	41%	4%
EGFR	89%	7%	4%	0%
p-EGFR	84%	16%	0%	0%
p-MAPK	31%	19%	38%	12%
p-STAT3	37%	22%	26%	15%
p-Akt	42%	35%	19%	4%

43 Sex Steroid Receptor, COX-2, and PAI1 Expression in Fibromatosis

JH Fasig, BW Whited, WD Dupont, SJ Olson, JM Cates. Vanderbilt University Medical Center, Nashville, TN.

Background: Although estrogen receptor-β (ER-β) and COX-2 expression have been demonstrated in fibromatosis, therapeutic responses using anti-estrogens and NSAIDs as single agents have been disappointing. Recently, plasminogen activator inhibitor-1 (PAI-1) and the androgen receptor (AR) have also been implicated in modulating the growth of fibromatoses. In this study, a series of deep and superficial fibromatoses were examined for expression of ER-β, ER-α, AR, progesterone receptor (PR), COX-2, and PAI-1.

Design: 27 cases of deep fibromatosis (excluding intra-abdominal cases) and 5 cases of the superficial variant were retrieved from the surgical pathology files at VUMC and used to construct a tissue microarray (TMA) for immunohistochemical analysis (IHC). For the steroid receptors, the number of positive nuclei were enumerated and scored as follows: 0, <5%; 1+, 5-33%; 2+, 34-66%; and 3+, >67%. Staining intensity for cytoplasmic or nuclear PAI-1 and COX-2 was also scored on a four-tiered scale. Results were correlated with disease-free survival using the log rank test and total tumor volume by one-way ANOVA.

Results: The IHC results for deep and superficial fibromatoses are presented in separate tables below. ER-β, AR, and COX-2 are present in most cases. As demonstrated previously, ER-α and PR were negative in all cases. PAI-1 was not detectable in any of the cases studied. None of the markers tested correlated with disease-free survival or total tumor volume.

Conclusions: Recently, molecular interactions between the AR and β-catenin have been characterized. Although not as well defined, cross-talk may also occur between Wnt pathway components and ERs. The co-expression of AR, ER-β, and COX-2 in fibromatosis suggests that hormonal manipulation therapy combined with COX-2 inhibitors may be beneficial in some patients. In contrast to a recent prior study, PAI-1 was not detected in the cases studied.

Deep Fibromatosis

	0	1+	2+	3+
AR	21%	21%	16%	42%
ER-α	100%	0%	0%	0%
ER-β	0%	0%	7%	93%
PR	100%	0%	0%	0%
COX-2	16%	36%	32%	16%
PAI-1	100%	0%	0%	0%

Superficial Fibromatosis

	0	1+	2+	3+
AR	0%	67%	33%	0%
ER-α	100%	0%	0%	0%
ER-β	0%	0%	0%	100%
PR	100%	0%	0%	0%
COX-2	20%	20%	60%	0%
PAI-1	100%	0%	0%	0%

44 *EGFR* Expression and Copy Number Gain Are Common in Pediatric Osteosarcoma Tumors

SS Freeman, SW Allen, R Ganti, J Wu, J Ma, X Su, GA Neale, JD Dalton, CA Billups, JS Dome, NC Daw, JD Khoury. St. Jude Children's Research Hospital, Memphis, TN.

Background: Although in vitro data from osteosarcoma cell lines demonstrate expression of the epidermal growth factor receptor (EGFR) and suggest that it might constitute a promising molecular target of therapy, no studies have systematically assessed the expression and genomic features of *EGFR* in osteosarcoma tumors.

Design: Eighty osteosarcoma tumor samples were included in this study. EGFR expression was surveyed by immunohistochemistry using tissue microarray sections. Immunostains were assessed for intensity (0: no immunostaining; 1: weak; 2: moderate; 3: strong) and percentage of at least 500 neoplastic cells exhibiting membranous or membranous and cytoplasmic immunostaining. EGFR expression was considered positive if the product of intensity and percentage was 20 or higher. Expression of EGFRvIII, a constitutively activated mutant form of EGFR with deletion of exons 2-7, was assessed by RT-PCR. The copy number status of EGFR was estimated using 50K Affymetrix SNP microarrays and fluorescence in situ hybridization (FISH). PCR amplification and sequencing were utilized to survey the EGFR tyrosine kinase domain for known activating mutations.

Results: EGFR expression was identified by immunohistochemistry in 23 of 28 (82%) osteosarcoma tumors. In 21 osteosarcoma tumors evaluated using RT-PCR and primers specific for *EGFR* exons 1 and 8, there was no evidence of EGFRvIII expression. Furthermore, mutation analysis of the EGFR tyrosine kinase in 32 osteosarcoma tumors revealed the presence of frequent polymorphisms but no evidence of known activating mutations. Notably, genotyping using SNP microarrays performed on 31 osteosarcoma tumor samples revealed frequent gains at the 7p11.2 locus. In 27 tumor samples, FISH showed evidence of EGFR amplification in 4 (15%), gain of material with chromosome 7 polysomy in 12 (44%), monoallelic loss in 1 (4%), and no copy number alterations in 10 (37%). Corresponding clinical information was available on 59 samples, which were derived from 59 patients (26 female; 33 male) with a median age of 14.1 years (range, 5-23 years). The median follow up duration for all surviving patients (n=41) was 4.4 years (range, 0.5-14). *EGFR* expression and copy number status did not correlate with clinical outcome.

Conclusions: EGFR expression and genomic gains at the *EGFR* locus are prevalent in pediatric osteosarcoma tumors. We found no evidence of EGFRvIII expression or activating mutations in the EGFR tyrosine kinase domain.

45 The Evaluation of Cell Cycle Proteins (CyclinD1, CyclinD3, P21, P27) and Ki-67 in Giant Cell Lesions of Bone

A Gokdemir, S Erdogan, M Ergin, S Ozbarlas, G Gonlusen. Cukurova University Medical School, Adana, Turkey.

Background: The cell cycle proteins have a crucial function in the transition between cycle phases. The alterations of these proteins have an important role in pathogenesis of several human tumors. In our study; we aimed to invastigate the similarity and differences of MN and giant cells with cell cycle proteins (cyclinD1, cyclinD3, p21, p27) and cell proliferation (Ki-67) in benign tumors of bone that have giant cells. Also the pathogenesis of giant cells have been evaluated.

Design: CyclinD1, cyclinD3, p21, p27 as cell cycle proteins and Ki-67 as a proliferation marker were applied by immunohistochemical method in seventy cases (18 giant cell tumor of bone, 15 aneurysmal bone cyst, 21 giant cell reperative granuloma, 16 giant cell tumor of tendon sheaths) that have been retrieved from the files.

Results: CyclinD3, p21 and p27 staining were similar for all cases. Positive staining with cyclinD1, cyclinD3, p21 and p27 in giant cells were found higher than mononuclear cells.CyclinD1 revealed negative staining in mononuclear cells of all giant cell tumor of tendon sheaths. Ki-67 staining was restricted in mononuclear cells of all cases. None of the cases showed positive Ki-67 staining in giant cells.

Conclusions: The numbers of positive staining with CyclinD1, cyclinD3, p21 and p27 in giant cells were found higher than mononuclear cells indicating that these cycle proteins may have a key role in giant cell differentiation. Mononuclear cells in giant cell tumor of tendon sheaths may have different immunophenotypical features than mononuclear cells of the other bone lesions because of negative cyclinD1 staining. Ki-67 staining was restricted in mononuclear cells of all cases and none of the cases showed positive Ki-67 staining in giant cells. This finding supported that giant cells do not have any proliferative activity. In conclusion, mononuclear cells are responsible for the proliferative activity and the cell cycle proteins are associated with the giant cell formation. Because of the osteolytic activity of giant cells, studies targeting these cycle proteins can provide non-surgical treatment opportunity.

46 Molecular Imaging of Multidrug Resistance in an Orthotopic Model of Osteosarcoma

CMF Gomes, M Welling, I Que, NV Henriquez, G van der Pluijm, S Romeo, AJ Abrunhosa, MF Botelho, PCW Hogendoorn, E Pauwels, AM Cleton-Jansen. LUMC, Leiden, Netherlands; IBILI, Coimbra, Portugal.

Background: Drug resistance is a significant obstacle to successful chemotherapy and constitutes a major prognostic factor in patients with osteosarcoma. Preliminary results obtained by our group have demonstrated that the sensitivity of osteosarcoma cell lines to cytotoxic drugs depends on multidrug resistant (MDR) related transporters and can be predicted based on functional assays using ^{99m}Tc-labelled Sestamibi. For *in vivo* recognition of MDR we developed an orthotopic model of osteosarcoma.

Design: Sensitive (143B) and resistant (MNNG) osteosarcoma cell lines expressing different levels of P-glycoprotein carrying a luciferase reporter gene were inoculated directly into the tibia of nude mice and local tumour growth was monitored weekly by whole-body bioluminescent reporter imaging (BLI) and by radiography. After development of tumours, dynamic images were acquired during 1 hour after injection of Sestamibi. A group of animals were pre-treated with a MDR-inhibitor (PSC833) before imaging. Images were analyzed for calculation of Sestamibi washout half-life ($t_{1/2}$), percentage of washout rate (%WR) and tumour/non-tumour (T/NT) ratio.

Results: A progressively increasing bioluminescent signal was detected in the proximal tibia after 2 weeks. Histological analysis demonstrated a high grade sarcoma morphologically consistent with osteosarcoma. Tumours were early detected after injection of Sestamibi and remained visible during the entire 4-5 weeks acquisition period. The $t_{1/2}$ of Sestamibi was significantly shorter in MNNG-tumours than in 143B-tumours. Administration of PSC833 increased significantly the retention in MNNG-tumours and had no significant effects on 143B-tumours.

Conclusions: The orthotopic injection of cancer cells provides a xenograft model closely resembling the clinical situation of osteosarcoma, and can be used for functional imaging of MDR. BLI detection of luciferase-transfected cells allowed the continuous non-invasive monitoring of tumour growth. The kinetic analysis of Sestamibi washout provides information on the functional activity of MDR-related to P-glycoprotein expression and its pharmacological inhibition. Therefore Sestamibi imaging might be a valuable clinical tool to predict chemotherapy response in osteosarcoma.

47 Primary Mediastinal Liposarcoma: Clinicopathologic Analysis of 24 Cases

HP Hahn, CDM Fletcher. Brigham and Women's Hospital & Harvard Medical School, Boston, MA.

Background: Although liposarcoma (LPS) is the most commonly occurring sarcoma in adults, liposarcoma arising in the mediastinum is rare and incompletely characterized in the literature.

Design: Twenty-four cases of mediastinal LPS were identified. 17 cases were from the consultation files of one of the authors, and 7 cases were from the surgical pathology files of Brigham and Women's Hospital. H&E sections were re-reviewed and clinical follow-up information was obtained from medical records or referring physicians.

Results: 13 patients were male and 11 were female. Patient age at time of diagnosis ranged from 3 to 72 years (mean 51). 21 patients were adults. 9 tumors were located in the anterior mediastinum, 7 in posterior mediastinum, 1 in superior mediastinum, and the precise location was not specified in 6 cases. Three of the anterior mediastinal tumors appeared to arise from the thymus. Grossly, tumors were well-circumscribed lobulated/multinodular masses measuring 2.2 to 61 cm in greatest dimension (median 16 cm). Cases included 10 well-differentiated liposarcomas, 8 de-differentiated LPS, 4 pleomorphic LPS, and 2 myxoid LPS. Of the well-differentiated LPS, 5 were adipocytic, 2 were spindle cell, 1 was the inflammatory variant, 1 had mixed adipocytic and spindle cell features, and 1 could not be subclassified. Of the pleomorphic LPS, 2 had areas mimicking myxofibrosarcoma with atypical hyperchromatic spindle and stellate cells in a myxoid stroma, but the focal presence of lipoblasts confirmed the diagnoses. Follow-up information was available in 15 cases (range 1-59 months; median 26). Complete resection was attempted in 14 cases. 5 patients developed local recurrence, including one patient whose tumor recurred twice. Two developed distant metastases (de-differentiated LPS: lung; pleomorphic LPS: liver and kidney). Eleven patients (5 well-differentiated LPS, 5 de-differentiated LPS, 1 myxoid LPS) were alive with no evidence of disease at last follow-up (mean 43 months). 1 patient remained alive with disease (pleomorphic LPS), 2 died of disease (pleomorphic LPS and de-differentiated LPS), and 1 died of unrelated disease.

Conclusions: Mediastinal liposarcoma appears to have similar epidemiologic, pathologic, and prognostic features as liposarcomas arising in the retroperitoneum. Mediastinal liposarcoma primarily affects middle-aged adults and is most commonly well-differentiated. Local recurrence is common and likely secondary to the difficulty of obtaining adequate surgical margins in this anatomic location.

48 An Orthotopic Animal Model of Osteosarcoma Metastasis: Comparison of Parental MG-63 Cell Line and Highly Metastatic Subclones

G He, HH Luu, XJ Luo, C Gong, E Bennet, K Sharff, MA Simon, TD Peabody, RC Haydon, MS Tretiakova, TC He, AG Montag. The University of Chicago, Chicago, IL.

Background: Osteosarcoma is the most frequent pediatric malignant bone tumor and has a high frequency of lung metastasis. To explore the mechanism of metastasis, a new orthotopic nude mouse model of metastasis was developed using intratibial injection. Using this model we compared parental and metastatic subclones of the MG-63 human osteosarcoma (OSA) cell line for motility, the ability to form metastatic foci, and the expression of ezrin, a cytoplasmic/membrane ERM family linking protein.

Design: An osteosarcoma cell line, MG-63, with low lung metastatic propensity was tagged with green fluorescence protein (GFP). The cell line was characterized *in vitro* and cell suspension was orthotopically injected into the right tibias of the nude mice. The mice were sacrificed at 6, 8, and 10 weeks. Radiographs and fluorescent whole body imaging were obtained and the lungs examined for metastases. The tissues were examined with H&E and immunohistologically with Ezrin. GFP tagged cells that metastasized to the lungs were recovered as cell lines, and parental line and metastatic subclone cell lines were compared for in-vitro growth and motility (Boyden chamber), in vivo metastatic efficiency and ezrin ezpression.

Results: Tumors were detected at the primary sites in the MG63 cells injected animals, but a very low incidence of spontaneous pulmonary metastasis was found up to 8 weeks following injection. In vivo comparison of metastatic efficiency showed a significantly higher incidence of lung metastases from the subclones as compared to the parental line. Interestingly, i*n vitro* comparison of motility and growth indicated that the parental MG63 cell line grew faster in a wound healing assay compared to the metastatic subclones. Immunohistochemical staining for ezrin was strongly positive with cytoplasm staining in all primary and metastatic tumors.

Conclusions: We have developed a clinically relevant orthotopic mouse metastasis model using an osteosarcoma cel line with low frequency of lung metastatis. Recovery of metastatic subclones selects for increased metastatic efficiency in the in-vivo system. This metastatic capacity does not appear to be correlated with a change in the expression of ezrin, nor with an increase in in-vitro growth and motility.

49 Epigenetic Alteration of p16 Is Involved in Dedifferentiation of Liposarcoma

M He, S Aisner, J Benevenia, F Patterson, T Lin, M Hameed. University of Medicine and Dentistry of New Jersey/New Jersey Medical School, Newark, NJ.

Background: Dedifferentiation of liposarcoma (DD) is a rare but not infrequent phenomenon where an atypical lipomatous tumor (ALT)/ well-differentiated (WD) liposarcoma shows abrupt transition to high-grade non-lipogenic sarcoma. The mechanism driving the progression is not clear. Methylation of p16 gene promoter has been reported in several solid tumors, including some WD liposarcomas. This study is aimed at understanding the role p16 gene promoter methylation in the dedifferentiation of liposarcoma.

Design: Out of 32 cytogeenetically confirmed ALT/WD liposarcomas from archives of UMDNJ- Pathology files, four cases were dedifferentiated liposarcomas (4/32, 12.5%). High quality DNA was available from paraffin-embedded blocks of both WD and DD component in 3 of the 4 cases. DNA was then modified using CpGenome™ DNA Modification Kit (S7820, CHEMICON International, Inc. Temecula, CA). Methylation status of p16 gene promoter was analyzed using methylation-specic PCR (MSP) followed by electrophoresis on 2% agarose gel. P16 expression was examined by immunohistochemical analysis on representative paraffin blocks from both components of the four dedifferentiated cases. As a control, four cases of WD liposarcoma with recurrence but without dedifferentiation were also stained for p16.

Results: Methylation of p16 gene promoter was seen in the DD component of two out of three cases (2/3, 67%), whereas the WD component of all three cases remained un-methylated (3/3, 100%). Both WD and DD components in all four cases (4/4, 100%) showed strong nuclear p16 expression without obvious difference of intensity between the two components. All four patients with recurrence of WD liposarcoma showed positive p16 expression (4/4, 100%) with same intensity between primary and recurrent tumors.

Conclusions: 1) P16 is involved in the pathogenesis of liposarcoma transformation 2) Epigenetic mechanisms such as methylation may play a role in tumor progression. 3) Methylation status study of p16 and related genes may provide prognostic value. 4) Methylation of p16 gene promoter by itself is not sufficient to abrogate protein production. Additional genetic changes such as loss of heterozygosity of p16 (usually not seen in liposarcomas) may be required.

50 Biotinyl-Tyramide-Based cRNA *In Situ* Hybridization: Application to *In Situ* Detection of SS18-SSX Transcripts in Synovial Sarcoma

M Hisaoka, A Matsuyama, H Hashimoto. School of Medicine, University of Occupational and Environmental Health, Kitakyushu, Fukuoka, Japan.

Background: cRNA *in situ* hybridization (ISH) is a robust molecular technique to examine both expression and localization of gene products of interest. Biotinyl-tyramide (BT)-based amplification has been recently employed to enhance signals in ISH and immunohistochemistry. It has not been, however, assessed if this approach is applicable to *in situ* detection of fusion gene transcripts as a diagnostic adjunct of fusion gene-associated soft tissue sarcomas such as synovial sarcoma.

Design: Digoxigenin-labeled cRNA probes flanking the fusion points of SS18-SSX1/SSX2 transcripts were synthesized by *in vitro* transcription. After a pretreatment with proteinase K, the probes were hybridized onto formalin-fixed, paraffin-embedded tissue sections of 14 synovial sarcomas and 4 other spindle cell tumors such as desmoid-type fibromatosis and solitary fibrous tumor. The hybridized probes were stringently washed and visualized with an HRP-conjugated anti-Digoxigenin antibody followed by BT and streptavidin-peroxidase complex. Integrity of RNA was assessed by ISH for products of phosphoglycerate kinase gene (PGK).

Results: In ISH for PGK, ten of the 14 synovial sarcomas showed detectable signals at least focally. Transcripts of the SS18-SSX1/SSX2 were identified in 11 cases including two PGK-negative ones. In nine fusion-positive cases, types of the SS18-SSX in ISH were concordant with those determined by fusion type-specific RT-PCR, although two examples showed signals of both probes probably due to their cross-hybridization. It was interesting to note that the signals were predominantly localized to epithelial components in three of the four biphasic tumors examined. Four spindle cell tumors other than synovial sarcoma were negative for the SS18-SSX despite detectable messages of PGK.

Conclusions: Our results suggest that BT-based ISH is another ancillary molecular technique for detection of SS18-SSX using formalin-fixed, paraffin-embedded tumor tissues. Expression of SS18-SSX may be associated with epithelial morphology of synovial sarcoma. To prevent cross-hybridization and improve the fidelity to fusion types in this system, more optimized conditions including appropriate stringent washes would be required.

51 Sclerosing Pecoma: Clinicopathologic Analysis of a Distinctive Variant with a Predilection for the Retroperitoneum

JL Hornick, CDM Fletcher. Brigham and Women's Hospital, Boston, MA.

Background: PEComas (tumors showing perivascular epithelioid cell differentiation) are a family of mesenchymal neoplasms that include angiomyolipoma, lymphangiomyomatosis, and a group of uncommon lesions that arise in visceral organs and soft tissue. We describe a distinctive variant of PEComa that shows extensive stromal hyalinization, a feature not previously described in these tumors.

Design: All extra-renal PEComas were retrieved from the authors' consult files. H&E sections were re-examined, immunohistochemistry was performed, and clinical details were obtained from referring physicians.

Results: 13 PEComas with extensive stromal hyalinization were identified from a total of 70 cases received between 1996 and 2006 (19%). All patients were female, with a mean age of 49 yr (range 34-73). One patient had tuberous sclerosis. 10 tumors (77%) arose in the retroperitoneum (8 pararenal), and 1 each in the pelvis, uterus, and abdominal wall. Mean tumor size was 12 cm (range: 4.5-28 cm). All except 1 were grossly well circumscribed. The tumors were composed of cords and trabeculae of cytologically uniform bland epithelioid cells with palely eosinophilic to clear cytoplasm and round nuclei with small nucleoli, embedded in abundant densely sclerotic stroma. 5 tumors contained a spindle cell component and 6 showed focally sheet-like areas. In all cases the tumor cells were focally arranged around blood vessels. All tumors lacked the delicate nesting vascular pattern typical of other PEComas. Mitoses ranged from 0-3 per 50 HPF (mean 1) in all cases except 1. One tumor showed abrupt transition to strikingly pleomorphic morphology, marked nuclear atypia, frequent mitoses (22/10 HPF), and fascicular and nested architecture. This was the only case with necrosis. All tumors were immunopositive for desmin (usually diffusely) and HMB45 (generally in scattered cells); 12/13 (92%) expressed SMA, 11/12 (92%) caldesmon, 11/12 (92%) microphthalmia transcription factor (D5), and 3/13 (23%) melan-A. Only 1 (8%) was focally S-100 positive. Follow-up ranged from 10-64 months (median 40). One patient (whose tumor showed transition to high grade malignant morphology) developed metastases to lung and liver. No other tumor has recurred or metastasized.

Conclusions: Sclerosing PEComa is a distinctive variant with a predilection for the pararenal retroperitoneum of middle-aged women. Sclerosing PEComas appear to pursue an indolent clinical course, unless associated with a frankly malignant component. Long-term follow-up will be required to confirm these findings.

52 Loss of INI1 Expression Is Characteristic of Both Conventional and Proximal-Type Epithelioid Sarcoma

JL Hornick, P Dal Cin, CDM Fletcher. Brigham and Women's Hospital, Harvard Medical School, Boston, MA.

Background: INI1 (hSNF5/SMARCB1), a member of the SWI/SNF chromatin remodeling complex located on chromosome 22q11, is deleted or mutated in strictly defined malignant rhabdoid tumors (MRT) of infancy. Recent studies suggest that some epithelioid sarcomas (ES) also show inactivation of INI1. However, very few cases of ES have been studied, and INI1 expression in other epithelioid malignant neoplasms has not been systematically examined. The purpose of this study was to evaluate the immunohistochemical expression of INI1 in ES compared to histologic mimics.

Design: 260 tumors were evaluated: 96 ES, including 47 conventional ("distal") ES, 44 proximal-type (PT) ES, and 5 with hybrid features of conventional and PT-ES; 53 metastatic carcinomas (21 from lung, 6 breast, 6 stomach, 5 colorectum, 5 kidney, 5 prostate, 5 pancreas); 12 metastatic testicular embryonal carcinomas; 20 metastatic melanomas; 20 epithelioid mesotheliomas; 20 epithelioid angiosarcomas; 10 epithelioid hemangioendotheliomas; 20 epithelioid malignant peripheral nerve sheath tumors (MPNST); 7 anaplastic large cell lymphomas; 5 histiocytic sarcomas; and 7 control MRT of infancy (4 brain, 2 soft tissue, 1 kidney). Immunohistochemistry was performed following pressure cooker heat-induced epitope retrieval using monoclonal antibody BAF47 (1:250; BD Biosciences). Fluorescence in situ hybridization (FISH) using probes directed against 22q11 was performed on isolated nuclei from 50 micron paraffin sections from 7 ES cases (3 conventional and 4 PT-ES).

Results: In total, 88 of 96 (92%) ES cases showed complete absence of INI1 expression, including 42 (89%) conventional ES, 41 (93%) PT-ES, and all 5 (100%) hybrid ES. Of the non-ES cases, 9 (45%) epithelioid MPNST also showed loss of INI1, as did all control MRT cases. INI1 expression was intact in all other tumor types examined. By FISH, abnormalities of 22q were detected in 2 of 3 conventional and 2 of 4 PT-ES cases.

Conclusions: Similar to MRT of infancy, loss of INI1 expression is characteristic of both conventional and PT-ES, being detected in greater than 90% of cases. These findings re-open the question of the possible relationship between ES, in particular PT-ES, and MRT. Nearly 50% of epithelioid MPNST are also negative for INI1. Immunostaining for INI1 can be used to confirm the diagnosis of ES in the appropriate context.

53 Well Differentiated Liposarcoma with Non-Lipogenic Spindle Cell Component: A Review of 33 Cases

Y Iwasa, Y Nakashima. Rakuwakai Otowa Hospital, Kyoto, Japan; Kyoto University Hospital, Kyoto, Japan.

Background: Well differentiated liposarcoma (WDL) and dedifferentiated liposarcoma (DDL) are well established entities in their classical forms. However, recent acceptance of low grade DDL and occasional events of co-mingling WDL and DDL components cause diagnostic difficulty, especially in the distinction between non-lipogenic spindle cell areas within WDL and DDL.

Design: 33 cases of WDL containing non-lipogenic spindle cell component w/o DDL between 1988 and 2005 in Kyoto University Hospital were reviewed. Fat amount, cellularity, proliferation pattern, nuclear atypia, mitotic counts, and transition between WDL and DDL were examined for each tumor.

Results: Patients age ranged from 20 to 79 years (mean 58.8 years), with M/F 1.75. 13 tumors arose in the retroperitoneum (39%), 10 in the limbs (30%), 5 in the paratesticular region (15%). The fat amount of the WDL was <5% in 13 cases, and 10-90% in 20 cases. All cases were grouped into the following 4 categories: WDL with focal non-lipogenic spindle cell component (WDL-FS) -3 cases (9%); DDL of non-lipogenic high grade sarcoma (classical DDL) -14 cases (42%); low grade DDL, characterized by moderately cellular bland spindle cell proliferation in a fascicular pattern (low DDL) -6 cases (18%); lipogenic differentiation within DDL of either low/high grade (co-mingling DDL) -10 cases (30%). Abrupt transition between WDL-FS and classical DDL was exclusive, whereas gradual or intermingled transition was predominant between WDL-FS and low or co-mingling DDL. Spindle cells in WDL-FS possessed hyperchromatic nuclei, more atypical than those in low DDL, and equivalent to those observed in classical DDL. Mitotic counts of both WDL-FS and low DDL were scarce (<1/10HPF), whereas those of classical DDL were numerous up to 15/10HPF. Follow-up information available for 22 patients (6 to 218 months) was variable and the above 4 groups revealed no apparent correlation with outcome.

Conclusions: 1) Low grade DDL and co-mingling DDL of both low and high grade are frequent and distinction from spindle cell areas of WDL may be arbitrary and subjective. 2) The overall outcome in our study showed no prognostic difference between WDL and DDL of low/high grade. 3) We suppose that atypical spinlde cells within WDL already obtain an aggressive biologic potential and in terms of biologic behavior, WDL should not be easily considered as low grade sarcoma.

54 Phospho-S6 Ribosomal Protein: A Potential New Predictive Sarcoma Marker for Targeted mTOR Therapy

OH Iwenofu, DG Goodwin, A Staddon, HM Haupt, JJ Brooks. Pennsylvania Hospital of the University of Pennsylvania Health System, Philadelphia, PA; Pennsylvania Hospital, Philadelphia, PA.

Background: Sarcomas are commonly chemotherapy resistant. mTOR (mammalian Target of Rapamycin), is a serine/threonine protein kinase of the phosphatidylinositol 3-kinase (PI3K)/Akt signaling pathway thought to have a key role in controlling cancer growth and thus an important target for cancer therapy (Rx). Several inhibitors of mTOR are in clinical trials; Ariad AP23573 is being tested on metastatic sarcoma. We hypothesized that a marker for the activity of the mTOR pathway (S6) would be predictive for the clinical response to the drug, that is, high tumor expression/activity would signify better response than low expression.

Design: In a blinded study of 26 patients treated, 21 remained on study and had available paraffin blocks. The S6 antibody (Cell Signaling Technology, 1/50 dilution) and the Ventana Benchmark XT automated stainer was used. Pretreatment biopsy or resection material was tested: the original tumor (7) or tumor recurrence/metastasis (14), either of which may have been post Rx with other agents. Tumors included: pleomorphic undifferentiated sarcoma (MFH, 5), osteosarcoma (3), leiomyosarcoma (5), liposarcoma (3); and 1 each of MPNST, malignant solitary fibrous tumor, synovial sarcoma, clear cell sarcoma, and sarcoma NOS. Staining was scored for quantity of tumor cells (%) and intensity (0, 1+ weak staining, 2+ intermediate staining, 3+ strong staining). Scoring was performed without knowledge of tumor response as either stable disease (S) or progressive disease (P).

Results: Staining quantity fell into 2 natural groups: high expressors (HE, ≥20%, 11 cases) and low expressors (LE, 0-10%, 10 cases). In the HE group, there were 9 S and 2 P cases (82% S); in the LE group, there were 3 S and 7 P cases (70% P). Chi-square

analysis had statistical significance (P≤0,05) at this blindly selected cutoff (10%). Since the only 2 progressors in the HE group had the lowest quantity scores (20, 25%), there might be justification for setting the cutoff at ≤25%; at that level, high S6 expression was strongly statistically significant for stable disease (P≤0.005).
Conclusions: The level of S6 expression was predictive of tumor response to the mTOR inhibitor. Phospho-S6 Ribosomal Protein is a promising new predictive sarcoma marker for targeted mTOR inhibitor therapy. Testing of a larger cohort in a prospective fashion is needed to further confirm clinical utility.

55 Grading of Soft Tissue Sarcoma in Children and Adolescents: Comparative Analysis of the POG and FNCLCC Grading Systems

JD Khoury, CM Coffin, JR Anderson, SL Spunt, JJ Jenkins, WH Meyer, DM Parham. St. Jude Children's Research Hospital, Memphis, TN; University of Utah, Salt Lake City, UT; University of Nebraska, Omaha, NE; University of Oklahoma, Oklahoma City, OK; University of Arkansas, Little Rock, AR.
Background: Two grading systems for soft tissue sarcoma (STS) are most widely used currently: the National Cancer Institute (NCI) and the Fédération Nationale des Centers de Lutte Contre le Cancer (FNCLCC) systems. Both were developed using cohorts of predominantly adult patients. The Pediatric Oncology Group (POG) system, based on the NCI system, has been proposed for grading pediatric STS. No systematic analysis of the applicability of the FNCLCC system in pediatric STS or its prognostic utility in comparison with the POG system has been undertaken.
Design: Histologic material from 133 patients with malignant non-rhabdomyosarcoma STS enrolled on three completed multi-institutional clinical trials were included in this study. Histologic grade was determined for each case pursuant to POG and FNCLCC grading criteria.
Results: Of 133 tumors, 105 (79%) were localized and 28 (21%) were metastatic. The estimated 5-year EFS for 130 patients with complete outcome data was 47%. As expected, stage and tumor size were highly predictive of EFS ($p<0.001$). The final grading results were as follows: 12 FNCLCC-G1; 75 FNCLCC-G2, 46 FNCLCC-G3; 4 POG-G1, 38 POG-G2, 91 POG-G3. Notably, both grading systems were highly predictive of EFS ($p=0.0095$ and $p=0.0075$, respectively). More cases were designated POG-G3 than FNCLCC-G3, and all cases designated FNCLCC-G3 were also POG-G3. Importantly, our data demonstrate that tumors graded POG-G3/FNCLCC-G2 (n=44) were associated with a more favorable outcome than those graded POG-G3/FNCLCC-G3 (n=44) and a less favorable outcome than those graded G1/G2 on both systems (n=42) ($p=0.0018$). This difference was also noted after adjusting for other risk features ($p=0.005$). Similar results were obtained when analyses were restricted to patients with non-metastatic disease.
Conclusions: Both the POG and FNCLCC grading systems provide an adequate prognostic measure of outcome for pediatric STS. However, a sizeable subset of cases with apparently intermediate prognosis was graded differently by the two systems. A larger prospective study might best address the proper grade assignment for such tumors.

56 Clinicopathologic Characteristics of Adult Primary Cardiac Sarcomas: Ten Year Experience with Analysis of 13 Cases

CH Kim, JY Dancer, MJ Reardon, QJ Zhai, AG Ayala, JY Ro. Weill Medical College Cornell University Medical College, The Methodist Hospital, Houston, TX; College of Medicine, Korea University, Seoul, Korea.
Background: Primary cardiac sarcomas are exceptionally rare. We present a 10 year, single institutional experience with thirteen primary adult cardiac sarcomas.
Design: Thirteen primary cardiac sarcomas were retrieved from the department pathology data file of the Methodist Hospital at Houston Texas. Clinical presentation and pathological features were analyzed. Histological classification was followed according to the criteria set by the World Health Organization (WHO), and grading according to the system proposed by the Federation Nationale des Centres de Lutte Contrele Cancer (FNCLCC).
Results: The median age of the patients was 39.7 years (range 19-68), and there were 8 men and 5 women (M: F=1.6:1). Eleven specimens were from surgically resected tumors, one was a postmortem sampling and one was from a complete autopsy. The tumors involved the right atrium (8), left atrium (2), right ventricle (2) and left ventricle (1). The tumor size ranged from 2.9 to 13.0 (mean 6.2cm) cm, and histologically there were 5 angiosarcomas, 5 unclassified sarcomas, 2 synovial sarcomas, and 1 leiomyosarcoma. All tumors were grade as 2 or 3 in differentiation. All five angiosarcomas were located in the right atrium (5/5) whereas 2 unclassified sarcomas were in the left atrium. No site of predilection was found for other histological types. The prognosis was poor with a median survival time of 13 months after diagnosis. There was no statistical correlation between survival and age, location, tumor type, or grade.
Conclusions: Angiosarcoma and unclassified sarcomas were the most common sarcomas of the heart accounting for 76%, but rare tumors such as synovial sarcoma and leimyosarcoma may also occur in this organ. The most common site was the right atrium, and the mortality rate was extremely high.

57 Hemizygous/Homozygous KIT Exon 11 Mutations Indicate Highly Malignant Clinical Behavior of Gastrointestinal Stromal Tumors (GISTs)

J Lasota, A Wlodarczyk, B Wasag, M Miettinen. Armed Forces Institue of Pathology, Washington, DC; Institute of Oncology, Warsaw, Poland; Medical University of Gdansk, Gdansk, Poland.
Background: GISTs are the most common mesenchymal tumors of gastrointestinal tract driven by gain-of-function KIT or PDGFRA mutations. GISTs range from benign indolent tumors to highly malignant sarcomas. Tumor size and mitotic activity are the best predictive prognostic features in GISTs. However, there is still a need to search for other additional prognostic markers.
Design: In this study, the clinicopathologic profile of GISTs with hemizygous/homozygous KIT exon 11 mutations was evaluated. Primary GISTs with such mutations identified by direct sequencing of PCR products were retrieved from AFIP KIT mutation database. In 17 cases normal tissue was available. In these cases, loss of heterozygosity (LOH) on chromosome 4 was evaluated using four microsattelite markers flanking PDGFRA-KIT region and 10 intragenic KIT-or PDGFRA-single-nucleotide-polymorphism (SNP) markers. Clinical data was obtained. All tumors included in this study were collected prior to tyrosine kinase inhibitor treatment.
Results: 28 of 700 (4%) GISTs from our database had hemizygous/homozygous KIT exon 11 mutations. Loss of multiple SNP- and LOH markers were found in all 17 cases analyzed suggesting that a great majority of these mutations has a hemizygous nature. 15 female and 13 male patients were included in this study. The pateint age varied from 37 to 80 years (median age 60 years). GISTs were diagnosed in stomach (n=13), small intestine (n=10), colon (n=2), rectum (n=1), and omentum (n=1). In 1 case, the location was unknown. The size of tumors ranged 3 from to 30 cm (average 12.4 cm), and 23 GISTs were >5 cm. Mitotic activity varied from 1 to 100 per 50/HPF (average 36 mitosis). Satisfactory follow-up data was available in 23 cases. 19 (82.6%) patients developed metastasis or died of the disease. The average survival time for 14 patients, who died of the disease, was only 30 months. Also, 5 GISTs diagnosed in patients without complete follow-up represented histologically malignant tumors.
Conclusions: A great majority of homozygous/hemizygous KIT exon 11 mutations diagnosed by direct sequencing of PCR products are hemizygous. Presence of such mutations in primary GISTs correlates with highly malignant course of disease and should be considered an additional prognostic marker.

58 Alveolar Soft Part Sarcoma: Review of 71 Cases Treated at a Single Institution

AJF Lazar, P Das, D Kotilingam, D Lopez-Terrada, C Warneke, D Lev. UT MD Anderson Cancer Center, Houston, TX; UTMDACC, Houston, TX; Texas Children's Hospital, Houston, TX.
Background: Alveolar Soft Part Sarcoma (ASPS) is a rare soft tissue sarcoma known to have a prolonged clinical course. It is associated with a recurrent translocation involving chromosomes X and 17 resulting in a fusion transcript involving the ASPL and TFE3 genes. We review the natural history of 71 cases seen at a single institution.
Design: Seventy-one histopathologically confirmed cases of ASPS treated at a single institution from 1976 to 2006 were reviewed and relevant clinical information obtained. Gathered information included the standard demographic data, primary and metastatic sites, size (cm), time to metastasis, treatment, and time of survival. Cox proportional hazard ratio methodology was employed to test for significant relationships.
Results: The reviewed histology was strikingly similar in all cases reviewed and revealed large discohesive epithelioid cells with abundant granular cytoplasm, central discohesion and surrounding thin vascular septae. Of the 71 patients, 59 % were male and 41 % were female and age at presentation ranged from 4 to 68 years (median, 31). Median follow-up was 9 years and with 31 % mortality. Primary sites included: extremity (69 %), head and neck (11 %), other (20 %). Primary tumor size ranged from 2 to 21 cm (median, 7). Number of metastases ranged from 0 to 12 (median, 2) and at least one metastatic focus was noted in the following sites: lungs (72 %), brain (34 %), other (20 %). Time to initial metastasis ranged from 0 to 239 months (median, 11 months). Recurrence of a primary tumor or metastatic site was very rare. Treatment was not uniform and included combinations of surgery, radiation and chemotherapy. Estimated median survival after primary diagnosis was 277 months. Only greater primary tumor size ($p=0.0117$) and shorter time to first metastasis ($p=0.0308$) were significantly associated with shorter survival. PCR amplification of the fusion transcript is currently in process for 35 cases where paraffin-embedded material is available to determine whether the type of fusion transcript (exon 2 or 3 of ASPL) or translocation (reciprocal or non-reciprocal) correlate with survival or other patient data.
Conclusions: ASPS is the only soft tissue sarcoma that commonly metastasizes to brain and is associated with prolonged survival despite multiple metastases.

59 Gene Expression Profiling of 24 Novel Sarcoma Cell Lines

CH Lee, S Zhu, M van de Rijn, JA Fletcher. Stanford University, Stanford, CA; Brigham and Women's Hospital, Boston, MA.
Background: Cell lines derived from fresh tumors have been widely used as experimental models but few sarcoma cell lines exist. Since the process of culturing may alter the phenotype of the cell, a careful molecular characterization of cell lines is useful to establish their validity. The aim of our current study is to examine the gene expression profiles of 24 novel sarcoma cell lines.
Design: Oligonucleotide arrays (HEEBO, Stanford) were used to characterize the global gene expression profiles of 24 sarcoma cell lines that included 4 rhabdomyosarcomas (RMS), 2 KIT-positive gastrointestinal stromal tumors (GIST), 1 KIT-negative GIST, 3 synovial sarcomas (SS), 3 malignant peripheral nerve sheath tumors (MPNST), 2 leiomyosarcomas (LMS), 2 liposarcomas (LPS), 2 endometrial stromal sarcomas (ESS), 1 Ewing sarcoma (EWS) and 4 undifferentiated sarcomas developed at Brigham and Women's Hospital. Gene array data from 16 fresh tumors (8 GIST and 8 SS) was included for comparison. Hierarchical clustering and significance analysis of microarray data (SAM) were used for data analysis.
Results: Unsupervised hierarchical clustering of the gene array data from the 24 sarcoma cell lines showed tumor-type specific co-clustering in 12 of the 20 cell lines of known sarcoma types in 3 of 4 RMS, 3 of 3 SS, 2 of 2 KIT-positive GIST, 2 of 3 MPNST and 2 of 2 ESS. SAM analysis of the cell lines also revealed gene expression profiles in accordance with data for fresh tumor samples. More significantly, in a separate unsupervised hierarchical clustering that combined the gene array data from 16 fresh tumors (SS and GIST) together with the 24 sarcoma lines, the 2 KIT-positive GIST cell lines clustered together with the 8 fresh frozen tissue GIST while all 3 SS clustered together with the 8 fresh frozen tissue SS.

Conclusions: The results of our gene expression analysis of the cell lines reveal that the majority of the 24 sarcoma cell lines exhibit distinct tumor-specific gene expression profiles that are in accordance with the current literature. The comparison of the cell lines and fresh frozen tumor tissues in the case of GIST and SS also indicate that defining gene expression properties of synovial sarcoma and GIST are well conserved in these cell lines, thereby making them highly representative experimental models.

60 Clinicopathologic, Immunohistochemical, and Biogenetic Analyses of Benign Versus Malignant Diffuse-Type Tenosynovial Giant Cell Tumors

CF Li, JW Wang, CC Tzeng, SC Chou, WW Huang, CN Lin, HY Huang. Chi-Mei Hospital, Tainan, Taiwan; Chang Gung Hospital, Kaohsiung, Taiwan; Veterans General Hospital, Kaohsiung, Taiwan; Tzu Chi Hospital, Dalin, Taiwan.

Background: Diffuse-type tenosynovial giant cell tumor (D-TSGCT), i.e., PVNS if intraarticualr, is a locally aggressive proliferation of synovial-like mononuclear cells with heterogeneous inflammatory infiltrates. Despite the discovery of *CSF1-COL6A3* gene fusion in benign lesions, the molecular aberrations accounting for malignancy in TSGCT remain unidentified.

Design: 3 primary and 2 secondary malignant D-TSGCTs, intraarticular in 1 and extraarticular in 4, were compared with 24 benign ones to assess clinicopathological differences. For 4 malignant cases with blocks, comparative genomic hybridization and immunohistochemistry (IHC) were performed to identify genomic imbalances and aberrant proteins implicated in sarcomatous transformation, using 8 and 24 benign cases for comparison, respectively. The IHC markers were Ki-67 and cell cycle regulators involving early G1 phase and G1/S transition, including cyclin D1, cyclin A, cyclin E, p53, p16, and p27.

Results: 5 malignant D-TSGCTs, affecting 3 females and 2 males, were 6 to 12 cm in size and located at or near the large joints (ankle, knee, wrist, suprapopliteal, and supracubital in 1 each). After diagnosis of malignancy, metastasis developed in one patient to lymph nodes and in another to the vertebrae, with latter patient eventually dead of disease. Old age, tumor necrosis, and higher mitotic count preferentially appeared in malignant D-TSGCT, but these were found in few benign cases. In contrast, only malignant D-TSGCT showed alteration in growth pattern ($p<0.001$), including histology of myxoid sarcoma, spindle cell sarcoma, and MFH in 1, 1, and 3 cases, respectively. Only cyclin A ($p<0.001$, 22.5±6.5% vs. 5.6±3.8%) and p53 ($p<0.001$, 23.8±14.9% vs. 3.8±2.7%) could robustly distinguish malignant from benign lesions without overlap in labeling indices between two groups. Genomic imbalances were only detected in malignant TSGCTs, which showed -2p, +3p, +6p, -9q, -10q, -14q, -15q, -16p, +18p, -18q, +19p, -20q, and -22q in various cases. Notably, -15q, the only recurrent alteration, was identified in 3, 2 of which showed identical deletions at 15q22-24.

Conclusions: Alteration in growth pattern is the most useful histologic feature to diagnose malignant D-TSGCT. Sarcomatous transformation of D-TSGCT is related to aberrations of cyclin A, p53, and chromosome 15q that may harbor a candidate tumor suppressor gene at 15q22-24.

61 Differential Expression of Syndecan-1 (CD138) in Myxoid Soft Tissue Tumors

J Liu, HM Haupt, JJ Brooks. Pennsylvania Hospital of the University of Pennsylvania Health System, Philadelphia, PA.

Background: Syndecan-1 (CD138) is a transmembane heparan sulphate proteoglycan expressed on both epithelial and mesenchymal cells. It functions in cell proliferation, migration, and cell-matrix interactions. Shift from syndecan-1 epithelial expression to stromal expression has been documented and is associated with poor tumor differentiation and invasion. Since myxoid stroma is known to be rich in heparan sulphate proteoglycans, we postulated that syndecan-1 may be expressed in some soft tissue myxoid neoplasms.

Design: 30 myxoid soft tissue tumors were selected: 9 myxofibrosarcomas (MYFS), 6 myxoid/round cell liposarcomas (M/RC LPS), 5 extraskeletal myxoid chondrosarcomas (EMC), 1 malignant myoepithelioma (MM), 4 aggressive angiomyxomas (AA), 3 myxomas (MYX), 1 chondromyxoid fibroma (CMF), and 1 neurofibroma with myxoid change (NFIB). Formalin-fixed, paraffin-embedded tissues were used for immunohistochemical staining with a prediluted mouse monoclonal anti-CD138/syndecan-1 antibody (B-A38, CellMarque) using the BenchMark XT; nodal plasma cells were the positive control. Staining intensity was scored as negative, 1+, 2+, 3+; staining distribution was recorded from ≤ 5%, ≤25%, ≤50%, ≤75%, and ≤100%; and the staining pattern (cytoplasmic and/or membranous) was noted.

Results: Syndecan-1 immunoreactivity was absent in all benign lesions (0/9). One third (33%) of malignant tumors were positive including 22% myxofibrosarcomas, 33% myxoid/round cell LPS, 40% EMC, and the one malignant myoepithelioma tested.

CD138 Expression in 30 Myxoid Soft Tissue Tumors

Tumor	no.	CD 138+	intensity	distribution	pattern
MYFS	9	2/9	2+, 3+	≤5%*, ≤100%	membranous, cytoplasmic*
M/RC LPS	6	2/6	3+	≤5%, ≤75%*	membranous, cytoplasmic*
EMC	5	2/5	3+	≤5%, ≤25%	membranous
MM	1	1/1	3+	≤5%	membranous
AA	4	0/4	0	0	0
MYX	3	0/3	0	0	0
CMF	1	0/1	0	0	0
NFIB	1	0/1	0	0	0

*cytoplasmic staining

Conclusions: CD138 was found to be differentially expressed among myxoid soft tissue tumors with only malignant tumors positive perhaps signaling an association with invasive potential. Its variable presence in both myxofibrosarcoma and myxoid/RC LPS limits its utility in this specific differential diagnosis. Further investigation of CD138 expression in myxoid neoplasms may lend insight into possible correlation with tumor aggressivity and prognosis.

62 Evaluation of CD99 Expression in a Large Series of Ewing's Sarcomas. The Experience of the PROTHETS Group

A Llombart-Bosch, MM Subramaniam, S Navarro, P Baccini, F Bertoni, N Savelov, JA Lopez-Guerrero. University of Valencia, Valencia, Spain; Istituti Ortopedici Rizzoli, Bologna, Italy; Blockin Cancer Center, Moscow, Russian Federation; Fundacion Instituto Valenciano de Oncologia, Valencia, Spain.

Background: The Ewing's sarcoma family of tumors (ESFT) is one of the most frequent solid neoplasms in pediatrics. These tumors share the presence of specific chromosomal translocations, which produce an *EWS/ets* gene rearrangement, as well as the expression, at extremely high levels, of CD99. This molecule modulates adhesion, apoptosis and differentiation of the carrying cells and constitutes a cardinal marker for the differential diagnosis of ESFT within round cell tumors. In addition, CD99 offers promising opportunities for new treatment strategies in these tumors. The aim of this study is to evaluate different commercial antibodies against CD99 in order to select the most suitable for the characterization of ESFT.

Design: We analyzed paraffin-embedded material from 150 ESFT subtyped as follows: 83 classic ES, 24 clear cell ES, 22 large cell ES, 10 PNET, 7 atypical ES, 3 spindle cell ES and 1 hemangioendothelial ES. Three tissue arrays (TA) of these cases were performed and immunohistochemical expression of CD99 was evaluated with four different commercial antibodies: HBA-71 (12E7, Dako Cytomation), O13 (Signet international), MEM 131 (Chemicon) and H036-1.1 (Biogene). All antibodies were optimized at 1/50 dilution in citrate buffer pH 6 with antigen retrieval.

Results: Expression of CD99 was observed in 97% of cases, the clone HBA71 (Dako cytomation) being the most sensitive marker in the diagnosis of ESFT. All positive cases for HBA71 in TA sections were in agreement with conventional full sections, and among the negative cases in TA (17%), only 6 cases (4%) were also negative in the full sections. The discordance rate of 17% was found to be due to either tumor heterogeneity or extensive necrosis in the tumor. The intensity of CD99 expression varies depending of ESFT variants. In this regard, PNET, atypical and clear cell ES express CD99 with less intensity. Interestingly, 3.6% of cases were negative for all types of CD99 antibodies.

Conclusions: The clone HBA71 was demonstrated to be the best and most sensitive marker in the diagnosis of ESFT and could be suitable for diagnostic and therapeutic purposes. Supported with grants FIS P1040822 Madrid, Spain and PROTHETS Contract number: 503036 of the FP6 from the European Commission.

63 Angioleiomyoma: A Clinicopathologic and Immunohistochemical Reappraisal with Special Reference to the Correlation with Myopericytoma

A Matsuyama, M Hisaoka, H Hashimoto. University of Occupational & Environmental Health, Kitakyushu, Fukuoka, Japan.

Background: In spite of the histological overlap, the relationship between angioleiomyoma and myopericytoma has not yet been fully evaluated. There have only been a few immunohistochemical studies on smooth muscle markers in angioleiomyomas. The aim of this study is to reappraise the tumors originally diagnosed as angioleiomyoma while paying special reference to the immunohistochemical expression of smooth muscle markers and a morphologic relationship to myopericytoma.

Design: One hundred thirty lesions originally diagnosed as angioleiomyoma and four tumors identified as myopericytoma were reassessed both histologically and immunohistochemically.

Results: One hundred twenty-two tumors were thus reclassified as angioleiomyoma (74 solid, 37 venous and 11 cavernous types) and 12 as myopericytoma based on the predominant histological pattern. In one patient, one myopericytoma and one venous type angioleiomyoma were synchronously present. The perivascular concentric arrangement of cells, that is a salient feature of myopericytoma, was also focally recognized in 19 angioleiomyomas (12 venous, four solid and three cavernous types). An angioleiomyoma-like fascicular pattern of elongated myoid cells was partially present in seven myopericytomas, four of which resembled the feature of the cavernous subtype and three the venous one. Immunohistochemically, most tumor cells of all cases of both angioleiomyomas and myopericytomas were diffusely positive for actins (alpha-smooth muscle actin and HHF35) and calponin, and all cases, except for one myopericytoma, were also diffusely or focally positive for *h*-caldesmon. Desmin was diffusely positive in 75.7% of solid type angioleiomyomas, 51.4% of venous type and 18% of cavernous type, whereas most of myopericytomas were negative for desmin, even though desmin-positive cells were only partially seen in three myopericytomas. The concentric structures of myoid cells in angioleiomyomas were, however, consistently negative for desmin.

Conclusions: Our study suggests that angioleiomyoma is therefore closely related to myopericytoma and the two types of tumors represent a morphologic continuum.

64 Detections of *FKHR* Gene Break-Apart by Fluorescence *In Situ* Hybridization (FISH) in Formalin Fixed Paraffin Embedded Alveolar Rhabdomyosarcoma

S Mehra, J Tull, A Shrimpton, G de la Roza, A Valente, S Zhang. SUNY Upstate Medical University, Syracuse, NY.

Background: Chromosomal translocations t(2;13)(q35;q14) and t(1;13)(p36;q14), resulting in *PAX3-FKHR* and *PAX7-FKHR* gene fusions, have been found to be specific molecular markers in most alveolar rhabdomyosarcomas (ARMS). Since the prognosis of ARMS is worse than that of embryonal rhabdomyosarcomas (ERMS), it is important to accurately distinguish these two subtypes. This distinction may be difficult on the basis of morphology alone when dealing with ARMS without characteristic alveolar pattern.

Design: To detect the genetic alterations of ARMS, "home brew" RT-PCR primarily on t(2;13)(q35;q14) or dual-color dual-fusion FISH have been used in most studies so far. In this study, we tested 20 cases of rhabdomyosarcoma (RMS) using a commercial *FKHR* gene break-apart FISH probe, which can detect both translocations involving the *FKHR* gene. The study included 6 cases of ARMS, 8 ERMS, 1 pleomorphic rhabdomyosarcoma, 5 rhabdomyosarcoma, not otherwise specified (RMS-NOS), and 10 other sarcomas. A home brew RT-PCR that could distinguish between the two translocations was also performed. Four pathologists independently reviewed all RMS without knowing the molecular findings. A consensus diagnosis was reached in all cases without unanimous agreement in the diagnosis. Histologic and molecular findings were correlated with clinical outcomes. The mean follow-up was 49 months (range from 2 to 185 months). For analytical purposes, the histopathologic diagnosis was used as the gold standard.

Results: All tested cases showed bright FISH signals with clear background. FISH was positive in four of six (66%) ARMS and 2 of 5 (40%) RMS-NOS. All other cases, including all ERMS, were negative. RT-PCR assay confirmed all FISH results. The 2 ARMS with negative FISH and RT-PCR showed characteristic alveolar features of ARMS. While two of six (33.3%) patients with positive FISH or RT-PCR died of the disease, there were no deaths among patients without these translocations.

Conclusions: The *FKHR* gene break-apart FISH probe is a simple and accurate tool to detect the translocations associated with ARMS. Despite two false negative ARMS cases by FISH and RT-PCR, there were no false positives among the ERMS cases. Since 40% of RMS-NOS cases in our study showed the characteristic genetic alterations of ARMS, FISH assay using a commercially available *FKHR* gene break-apart probe provides an additional useful tool in the diagnosis of rhabdomyosarcomas and an alternative to RT-PCR.

65 Insulin-Like Growth Factor (IGF)-I and IGF-I Receptor (IGF-IR) Are Consistently Expressed in Soft Tissue Liposarcomas

T Mitsuhashi, M Watanabe, H Sasano, M Ono. Tohoku University Graduate School of Medical Science, Sendai, Miyagi, Japan; Tohoku University Hospital, Sendai, Miyagi, Japan.

Background: IGF system has been implicated in tumor development and progression in various neoplasms including osteogenic and soft tissue sarcomas. IGF-I and II are coded for by separate genes and bind to specific cell surface receptors, eliciting a mitogenic response. Transforming growth factor(TGF)-β work either synergistic or down-regulatory depending on tumors. Many of liposarcomas contained elevated IGF-I and II messenger RNA levels, while control adipose tissue contained very low or undetectable levels (Tricoli JV, et al. Cancer Res. 1986). Accordingly, IGF-I seems to involve in tumor growth and development of liposarcomas; however, no immunohistochemical studies have been reported regarding the expression of IGF-I and IGF-IR in liposarcomas.

Design: We investigated 183 bone and soft tissue tumors in total. Formalin-fixed, paraffin-embedded tissues were used in this study. Immunohistochemical studies for IGF-I, IGF-IR, and TGF-β on these tumors were performed with or without antigen retrieval. After screening of immunohistochemical staining in all of the above tumors, then we focused on 47 patients (mean age 59.6 years, M:F=25:22) with liposarcomas (29 well differentiated, 10 myxoid/round, 3 pleomorphic, 2 dedifferentiated, and 3 mixed) who underwent surgical resection.

Results: Among 183 bone and soft tissue tumors, only chordomas and liposarcomas showed consistent expression of IGF-I. The results of chordomas were previously presented [Mod Pathol 2006;19:6(Suppl 3)]. More than 90% of liposarcomas we examined showed immunohistochemical expression of IGF-I. Well-differentiated and mixed types were almost always positive for IGF-I and IGF-IR. TGF-β was positive for either in tumor cells and/or endothelial cells. The results of the IGF-I expression in myxoid/round cell and pleomorphic liposarcomas were various (7 positive, 3 weakly positive, and 3 negative). One dedifferentiated liposarcomas were focally positive for IGF-I and the other was negative.

Conclusions: Well-differentiated liposarcomas showed consistent expression of IGF-I and IGF-IR; however, liposarcomas with higher grades showed various expression of these molecules. Although MDM2 and CDK4 amplification have been known in these tumors, other mechanisms related to IGF-I may exist for tumor growth and development of liposarcomas. This is the first immunohistochemical study for IGF-I and IGF-IR expression in liposarcomas.

66 Phosphorylated H2AX Expression in Osteosarcoma and Selected Primary Bone Tumors

AG Montag, G He, S Chmura, A Khramtsov, M Tretiakova. University of Chicago, Chicago, IL.

Background: H2AX is a unique isoform of the histone H2A that is phosphorylated by the kinases ATM, ATR among others in response to double stranded DNA (dsDNA) breaks. Phosphoryalted H2AX (pH2AX) co-localizes with and provides a scaffolding for many of the components of DNA damage response, including BRCA1. Immunostaining for pH2AX is stoichiometrically proportinoal to the number of dsDNA vreaks present, and has been used to approximate DNA damage from radiation. The present study examines a series of pretreatment osteosarcomas and benign bone tumors to test whether the cytogentic and genomic instability seen in osteosarcomas is reflected by pH2AX staining.

Design: Pretreatment biopsies from primary bone lesions were retrieved from the paraffin archive and included 35 osteosarcomas, 4 Ewing's sarcoma and 14 benign bone lesions: (4 giant cell tumors, 6 aneurysmal bone cysts, 2 chondroblastomas and 2 osteoid osteomas). Five micron sections underwent microwave retrieval and immunostaining with antibody to pH2AX (Cell Signalling). Controls included irradiated mouse tissue and a mouse embryonic fibroblast xenograft previously knocked out for H2AX expression. Staining was scored as 0, 1+ (less than 5% of nuclei), 2+ (5 to 19% of nuclei) and 3+ (greater than 20% of nuclei). Obvious areas of necrosis or apoptosis were excluded from analysis.

Results: 31 of 35 osteosarcomas showed pH2AX staining, 22 of 25 at 2 to 3+ intensity. There appeared to be no trend in staining by histologic subtype of osteosarcoma. All benign bone lesions were negative for pH2AX staining, as were the majority of Ewing's sarcoma cases. Occasional apoptotic cells or degenerating mutinucleated giant cells demonstrated staining in all lesions.

Conclusions: pH2AX staining is present in pre-treatment osteosarcomas, indicating that dsDNA breaks are indigenous. The absence of pH2AX staining in benign lesions and in Ewing's sarcoma, which has a more stable karyotype, suggests that H2AX staining is an indicator of accumulated unrepaired DNA damage and genetic instability in osteosarcoma.

pH2AX Staining Intensity in Bone Tumors

	0	1+	2+	3+
Osteosarcoma (n=35)	4	9	10	12
Ewing's Sarcoma (n=4)	3	1	0	0
Aneurysmal Bone Cyst (n=6)	6	0	0	0
Chondroblastoma (n=2)	2	0	0	0
Giant Cell Tumor(n=4)	4	0	0	0
Osteoid Osteoma (n=2)	2	0	0	0

67 Desmoplastic Fibroma: More Clearly Defining This Entity. A Clinicopathologic and Radiologic Study of 58 Cases

CA Moran, JA Vidal, MD Murphey, M Miettinen, JC Fanburg-Smith. MD Anderson Cancer Center, Houston, TX; Armed Forces Institute of Pathology, Washington, DC.

Background: There are only few older series reported on desmoplastic fibroma (DF), considered the bone counterpart of fibromatosis (desmoid). DF is encountered mostly in the mandible and long bones, in the second decade, and may be locally aggressive, yet benign. Newer information reveals their potential lack of beta-catenin expression, unlike desmoid. We wanted to clinicopathologically and radiologically review our cases of this rare entity, the largest series to date.

Design: All available radiologic, clinical, and pathologic material from 112 cases coded as DF were reviewed. Those cases with insufficient material or better diagnosed as other entities, including fibromatosis, fibrous dysplasia, and a hypocellular region of intraosseous fibrosarcoma, were excluded from this study. Immunohistochemical stains (IHC), clinical history, and radiologic images were obtained and reviewed.

Results: 58 cases were included: 33 M: 24 F: 1 unknown gender. Ages ranged from 3-75, with a median of 24 years. The most common sites involved the following bones, in decreasing order: femur, maxilla/mandible, tibia, pelvis, humerus, rib, foot, ulna, fibula, vertebra, frontal, clavicle, and scapula. Tumor sizes ranged from 2.5 to 14 cm. Radiologically, these DF were mostly lytic, expansile, intraosseous, and metaphyseal with only a few cases demonstrating pathologic fracture. 5% of cases had a small soft tissue component, mostly when the cortex was fractured. Most outside radiologic diagnostic considerations were malignant. Pathologically, most cases invaded cortex and created adjacent new bone formation but did not involve soft tissue. The tumors were without neoplastic bone; endochondral ossification only noted at fracture sites. DF were low to moderately cellular, with spindled to ovoid cells, often arranged in a storiform pattern. Vessels were mostly obscured and not obviously elongate. Focal perivascular microhemorrhage, myxoid change, and keloidal collagen were observed. Initial IHC panel reveals DF to be negative for nuclear beta-catenin, ER/PR, desmin, S100 protein, keratins, CD117, PDGFRA, and CD34, the latter two ruling against relationship to DFSP.

Conclusions: While focal DFlike areas can be seen in other tumors, DF appears to be a distinctive intraosseous entity and is truly separate from desmoid (fibromatosis) and other fibroblastic tumors clinically, radiologically, morphologically, and immunogenetically.

68 Comprehensive Detection of Gene Fusions in Sarcomas and Other Cancers Using Exon-Level Expression Data Obtained by Affymetrix Exon Arrays

T Motoi, N Socci, A Lash, F Mertens, W Gerald, M Ladanyi. Memorial Sloan-Kettering Cancer Center, New York, NY; Lund University Hospital, Lund, Sweden.

Background: Specific gene fusions represent, in terms of numbers of different genes involved, the single most common type of somatic genetic alteration in human cancer but there has so far been no feasible way to screen for this major class of genetic alterations. Because most gene fusions that lead to the formation of a chimeric protein cause an intragenic discontinuity in the RNA expression levels of the exons that are 5' or 3' to the fusion point in one or both of the translocation partners, we examined whether the new Affymetrix Exon arrays could detect such change points in the exon level expression data to allow an unbiased comprehensive screen for cancer fusion transcripts.

Design: To develop the approach, Affymetrix Exon array hybridizations were first performed on samples with known gene fusions including sarcoma cell lines, sarcoma primary tumor RNAs, and other types of samples with fusions (leukemias, prostate cancer). For each sample, the expression levels of the 3' exons included in the expected fusion transcripts were compared to the distribution of exon expression levels in Exon array data from normal and neoplastic samples known not to contain that fusion.

Results: For many fusions, there was a clear disparity in the expression levels of 5' and 3' exons and the change point matched the known exon structure of the fusion transcript in that sample. For instance, this was the case for some or all samples with *EWS-WT1*, *EWS-ATF1*, *EWS-FLI1*, *EWS-ERG*, *SYT-SSX1*, and *TMPRSS2-ERG* (prostate CA). To

identify fusion transcripts in an unbiased fashion, a heuristic score (a statistical score algorithm designated "the fusion score") was developed to quantify the discontinuity in an individual sample's exon expression levels versus the expected variation in negative control samples without known fusions. This fusion score algorithm identified samples with *EWS-WT1* and *SYT-SSX1* as clear outliers, suggesting that the approach should be able to identify fusion transcripts without any prior knowledge of the genes involved.
Conclusions: Known gene fusions in sarcomas and other cancers can be detected by the exon-level expression data provided by Affymetrix Exon arrays, in both cell lines and tumor samples. The application of this approach to the discovery of novel gene fusions is of obvious interest and is being pursued.

69 Epithelioid Hemangioma of Bone. A Study of 39 Cases

GP Nielsen, A Srivastava, JX O'Connell, C Mangham, AE Rosenberg. Massachusetts General Hospital, Boston, MA; CJ Coady Assoicates, Surry, BC, Canada; Royal Orthopaedic Hospital, Birmingham, United Kingdom.
Background: Epithelioid hemangioma (EH) is a distinct clinicopathologic entity that most frequently arises in the skin and soft tissues. However, it has been reported to develop in a variety of different sites including the skeleton where it is often confused with malignant endothelial neoplasms. In fact, some investigators believe that this tumor does not exist in bone and should be classified as a form of hemangioendothelioma or low-grade malignancy. To further study the clinical behavior of these tumors we report our experience with 39 epithelioid hemangiomas of bone.
Design: 39 osseous EHs were retrieved from the consultation files of two of the authors (AER, JXO) and the pathology files of the participating institutions. Treatment and follow information was obtained from the medical records, treating physicians and referring pathologists.
Results: The study group included 22 males and 17 females, whose ages ranged from 10-69, (mean 38) yrs. The tumors were located mainly in tubular and flat bones and measured up to 15.0 cm (range 1 to 15 cm). 5 patients had multifocal disease at presentation. The tumors had a lobular architecture and all contained well-formed blood vessels lined by prominent epithelioid endothelial cells. In many cases the epithelioid endothelial cells grew in solid sheets. Tumor cells had abundant eosinophilic cytoplasm that sometimes contained round clear vacuoles and large vesicular nuclei with conspicuous nucleoli. Nuclear atypia was limited. In some cases the stroma contained a prominent inflammatory infiltrate rich in eosinophils – no hyalinized myxoid ground substance was present in any tumor. All patients were treated by resection or curettage. Follow up information available on 29 patients ranged from 6 to 276 months. Four patients developed local recurrence and in one of them a small deposit of tumor was seen in a regional lymph node. None of the patients died of disease, including the patient with lymph node involvement who is alive and well with no evidence of disease 38 months later.
Conclusions: EH of bone is a benign neoplasm that has distincitive clinical and morphologic features. EH may be multifocal and locally recur in a minority of cases. Accordingly, we recommend that it be treated with curettage or limited local resection in appropriate cases.

70 Dermatofibrosarcoma Protuberans *COL1A1-PDGFB* Fusion Is Identified in Virtually All DFSP Cases When Investigated by Newly Developed Multiplex RT-PCR and FISH Assays

KU Patel, SS Szabo, V Prieto, AJF Lazar, DH Lopez-Terrada. Baylor College of Medicine, Houston, TX; MD Anderson Cancer Center, Houston, TX.
Background: Dermatofibrosarcoma protuberans (DFSP) and its juvenile variant giant cell fibroblastoma (GCF) are cutaneous locally aggressive spindle cell tumors of intermediate malignancy. Tumor cells are reactive for CD34 and characterized by a t(17;22) or supernumerary ring chromosome resulting in the fusion of exon 2 of *PDGFB* to various exons of *COL1A1* gene. We developed a multiplex reverse transcription PCR (RT-PCR) assay to detect fusion transcripts for the numerous possible *COL1A1* breakpoints. 27 formalin-fixed, paraffin embedded (FFPE) DFSPs and GCFs were analyzed and results correlated with histology, immunohistochemistry, FISH analysis and cytogenetics.
Design: 25 DFSPs and 2 GCFs were reviewed by two soft tissue pathologists. Multiplex RT-PCR was performed on FFPE tumor tissue using 18 forward primers spanning the α-helical domain of *COL1A1* gene and 1 reverse primer for exon 2 of *PDGFB* gene. Forward primers were validated using reverse primers for various exons of the *COL1A1*gene, tested using control RNA. Sequence analysis of PCR products was performed to characterize breakpoints. Results were validated using a *PDGFB* direct labeled, break-apart FISH probe.
Results: Fusion transcripts were detected in all but 1 DFSP and none of 2 GCF cases suitable for PCR analysis. Conversely a *PDGFB* rearrangement was detected by FISH in one GCF case. Sequence analysis revealed a *PDGFB* breakpoint in exon 2 in all cases. *COL1A1* breakpoints were in exons 7 (1 case), 10 (1), 26(2), 29 (3), 33 (1), 40 (1), 43 (7), 45 (1) and 46 (3). Three novel *COL1A1* breakpoints were identified, in exons 13 (1), 30 (1) and 49 (2).
Conclusions: We developed a multiplex RT-PCR-direct sequencing assay for FFPE tissue to study the prevalence of COL1A1-PDGFB fusion transcripts and *COL1A1* breakpoint variants in DFSP and GCF. Fusion transcripts were identified in all DFSPs but 1 and none of 2 GCFs. Three novel *COL1A1* breakpoints were documented. There was no correlation between breakpoints and age, sex or histologic variants. A *PDGFB* rearrangement was identified in a GCF case negative by RT-PCR, suggesting the possibility of an alternate partner gene. Using this sensitive RT-PCR assay in combination with FISH, *COL1A1-PDGFB* rearrangements appear more prevalent in DFSP than previously reported. Its detection may be particularly helpful in the differential diagnosis of atypical, fibrosarcomatous and metastatic DFSP.

71 Are Post-Irradiation Atypical Vascular Lesions Associated with Angiosarcoma? An Analysis of 27 Cases

KT Patton, AT Deyrup, SW Weiss. Emory University School of Medicine, Atlanta, GA.
Background: "Atypical vascular lesion" (AVL) is a term used for post-irradiation cutaneous vascular proliferations that possess some, but not all, of the features of angiosarcoma. Most occur in women following lumpectomy and radiation for breast carcinoma. Given the limited published data, it is still unclear whether AVLs are innocuous, incidental lesions or a risk factor / precursor lesion for angiosarcoma, and, if the latter, the extent of the risk.
Design: Twenty-seven AVLs occurring in the skin of the breast following lumpectomy and radiation therapy for breast carcinoma were reviewed. All had been referred in consultation in order to exclude angiosarcoma.
Results: The patients, all women, (age 41-95 yrs; mean 64 yrs) presented with 1 or more small papules (n=15) or plaques (n=5) which measured from 1.5 mm-10 mm (mean 3.7 mm) and that occurred subsequent to radiotherapy (range 3-12 yrs; mean 5 yrs). Histologically the lesions could be divided into two groups: a lymphatic type and a vascular type. The lymphatic type (LT) (n=18) consisted of a proliferation of benign-appearing, ectatic, variably anastomosing lymphatic vessels that were usually restricted to the superficial dermis (n=14) but occasionally extended to deep dermis (n=3) or subcutis (n=1). The vascular type (VT) (n=8) consisted of ramifying, non-ectatic, capillary vessels lined by a single layer of endothelium and typically involved deep dermis and subcutis (n=7) but rarely were confined to the superficial dermis (n=1). One lesion had features of both LT and VT. Patients were treated by biopsy alone (9), re-excision (9), mastectomy (3) or unknown procedure (6). Clinical follow-up was obtained in 21 cases (range 4-105 months; mean 34 months): 19 patients were alive without disease; 1 patient with VT developed angiosarcoma within 14 months of biopsy and 1 patient died of other causes and without disease at 40 months.
Conclusions: AVLs embrace a spectrum of changes ranging from banal, superficial lymphatic proliferations to deep, more complex lymphatic and capillary vascular proliferations. There appears to be some association of AVL with angiosarcoma which may differ depending on the type (i.e. histologic features) of AVL. Future outcome studies of AVL should take these differences into account.

72 Is Better Chemotherapy Response in Telangiectatic Osteosarcoma Due to Increased Tumor Vascularization or Higher Proliferation Index? A Comparative Immunohistochemical Study of 20 Cases

L Rezeanu, AC Baker, GP Siegal, MJ Klein. University of Alabama at Birmingham, Birmingham, AL.
Background: Telangiectatic osteosarcoma accounts for less than 4% of all osteosarcomas. If not treated chemotherapeutically, it is thought to have a worse prognosis than the conventional type. However, recent studies suggest that, with adjuvant chemotherapy, its prognosis is identical to or better than conventional osteosarcoma. Radiographic studies demonstrate a purely lytic destructive lesion without matrix mineralization. Grossly, it is characterized by large blood-filled spaces with or without intervening septa. Histologically, the tumor is comprised of osteoid producing malignant cells present at the periphery or within the tumor septa.
Design: Studies of the susceptibility of telangiectatic osteosarcoma to neoadjuvant chemotherapy correlated with disease free survival times demonstrated the exquisite chemosensitivity of this tumor. One hypothesis explaining this finding is increased tumor vascularity with better drug penetration. However, a known chemotherapeutic effect, documented by serial angiography studies, is reduced vascularization of the tumor bed contradicting the aforementioned hypothesis. In our study, the expression of Ki67 and CD31 in 10 cases of telangiectatic osteosarcoma was compared to 10 cases of conventional osteosarcoma. The immunostains were performed on pretreatment, diagnostic biopsies. The proliferation index was determined by counting the number of Ki67 positive cells to 100 cells in 10 high power fields. The average of the values obtained was expressed as percentage of positive cells. The degree of vascularization was evaluated by counting the number of CD31 positive microvessels in 3-4 "hot spots" (areas of increased vascularity), according to an international consensus report (Vermeulen, et al) and calculating the mean value. The proliferation index and degree of tumor vascularization were compared between the two groups.
Results: Preliminary results show that the proliferation index is significantly higher in telangiectatic compared to conventional osteosarcoma ($p < 0.05$), whereas the vascular pattern is not significantly different ($p > 0.05$). This supports a novel paradigm explaining the response to chemotherapy of telangiectatic osteosarcoma, taking into account that the chemotherapeutic drugs used in most treatment regimens target DNA in actively proliferating cells.
Conclusions: We conclude that telangiectatic osteosarcoma remains a suitable tumor for drugs which target cell proliferation.

73 Peroxisome Proliferator Activated Receptor Gamma (PPAR-γ) Expression in Dedifferentiated Liposarcoma: Comparison of Well-Differentiated and Dedifferentiated Components

JT Schaefer, C Lee, MJ Kramer, RJ O'Donnell, AE Horvai. UCSF, San Francisco, CA.
Background: The mechanisms of sarcoma progression are poorly defined, in part because the precursor lesions of most sarcomas are unknown. Liposarcoma represents a unique model insofar as progression from well-differentiated liposarcoma (WL) to de-differentiated liposarcoma (DL) is a well-documented process. The progression to DL, marked by a loss of lipogenic differentiation, confers metastatic potential and a worse prognosis. Peroxisome proliferator activated receptor gamma (PPAR-γ) is a nuclear hormone receptor that plays a critical role in adipocyte differentiation. Prior

studies have demonstrated PPAR-γ mRNA in various subtypes of liposarcoma. Further, terminal adipocyte differentiation can be induced in myxoid/round cell and pleomorphic liposarcoma in vivo by a PPAR-γ agonist. However, alterations, if any, of PPAR-γ, expression during the progression from WL to DL remain to be described.
Design: The purpose of this study was to determine whether PPAR-γ immunoreactivity is altered during the progression from WL to DL and whether the immunoreactivity correlates with grade of the DL component or clinical parameters. We identified 28 cases of DL (22 primary, 6 secondary) by histology. Tissue was immunostained with an antibody to PPAR-γ using standard methods. Cases with ≥10% of cells showing specific, strong, nuclear staining were considered positive and stratified on the percent of cells staining. Staining results were compared between corresponding pairs of WL and DL and stratified based on grade of DL, presence of metastasis and clinical presentation.
Results: 26 of 28 cases (93%) of DL showed specific nuclear staining for PPAR-γ but no significant difference (p=0.08) was noted in staining score between paired well-differentiated and de-differentiated components. No significant correlation (p> 0.4, respectively) was observed between PPAR-γ staining and the grade of DL, metastasis or presentation (primary or secondary).
Conclusions: The majority of DL express PPAR-γ in both the well-differentiated and de-differentiated components suggesting that PPAR-γ expression is not altered during progression to DL. Furthermore, PPAR-γ expression is largely retained regardless of the grade of the dedifferentiated component. Consequently, receptor-targeted therapeutics may be a useful adjuvant strategy in the treatment of DL.

74 EXT and Its Downstream Targets in Central Chondrosarcoma (CCS)

YM Schrage, L Hameetman, K Szuhai, AM Cleton-Jansen, AHM Taminiau, PCW Hogendoorn, JVMG Bovée. LUMC, Leiden, Netherlands; Leiden University Medical Center, Leiden, Netherlands.
Background: CCS grows in the medullar cavity of bone and is the most common CS subtype. Enchondromas (EC) are benign tumors at this location. In contrast to peripheral CS (PCS), which develops at the bone surface within osteochondroma, little is known about the genetic background of CCS. Homozygous mutations of the *EXT1* and *EXT2* tumor suppressor genes cause solitary and hereditary osteochondromas. The EXT1/EXT2 protein complex is involved in biosynthesis of heparan sulphate proteoglycans that function in gradient formation of Indian hedgehog (IHH), WNT and TGF-β. These activate PTHLH signaling, controlling chondrocyte proliferation and differentiation in the normal growth plate. Moreover, PTHLH signaling is involved in chondrocyte proliferation in both PCS and CCS.
Design: To study EXT and its downstream signaling pathways in CCS we studied expression of *EXT* in EC (n=7) and CCS (grade I n=11, grade II n=7 and grade III n=9) by qPCR. DNA of 2 CCS with decreased *EXT* expression was hybridized on an 8q CGH tiling array. The downstream targets of IHH signaling, *PTCH*, *SMO* and *GLI2*, were investigated by qPCR. Immunohistochemical analysis for β-catenin, phosphosmad-2 and PAI-1 were performed on 76 tumors, to study WNT and TGF-β signaling.
Results: *EXT* mRNA levels in tumors were comparable to growth plates. Only two of 34 tumors showed decreased *EXT1* expression, without alterations in the 8q24 region shown by array-CGH. IHH signaling is active since *PTCH*, *SMO* and *GLI2* were expressed as in normal growth plates. 5/20 EC and 19/56 CCS showed nuclear localization of β-catenin, suggesting active WNT signaling. All tumors were positive for phosphosmad 2. PAI-1 immunohistochemistry showed positivity in 24/33 EC, 20/27 low-grade and all 29 high grade CCS, indicating active TGF-β signaling.
Conclusions: While *EXT1* expression in PCS is decreased due to mutations, we show that most CCS have normal *EXT* mRNA levels. In contrast to the homozygous loss of EXT1 that we previously showed in osteochondroma, genomic alterations in the EXT region were absent in two CCS with diminished *EXT* expression. WNT signaling is probably active in a subset of both CCS and PCS. While chondrocyte proliferation by PTHLH signaling is activated by IHH signaling in low-grade PCS and overtaken by TGF-β signaling in high grade PCS, we show that in CCS, both pathways are active, irrespective of histological grade and are candidates to stimulate PTHLH.

75 Actinin-4 Expression in 187 Cases of Gastrointestinal Stromal Tumor (GISTs) of the Stomach and Intestine: An Immunohistochemical (IHC) Study

K Seki, K Honda, T Yamada, U Yamaguchi, Y Suehara, T Shimoda, T Hirohashi. National Cancer Center Hospital, Tokyo, Kazakhstan; National Cancer Center Reserch Insutitute, Tokyo, Japan.
Background: Enhanced motility of cancer cells by remodeling of the actin cytoskeleton may crucial in the process of local invasion and distant metastasis. We previously identified an actin-binding protein, actinin-4, is a new biomarker of cancer invasion and an indicator of prognosis for patients with breast and colorectal cancer (J Cell Biology 1998;140:1383, Gastroenterology 2005;128:51). This study assessed the role of actinin-4 in the motility and metastatic potential of GISTs.
Design: 187 cases of GISTs were assessed by IHC with an actinin-4 polyclonal antibody. We analyzed the actinin-4 expression with clinical features and risk classification of GIST determined by tumor size, necrosis, mitosis, and MIB-1 score as well as clinical outcome. Intensity of actinin-4 staining was divided into a high group and a low group based on a actinin-4 staining of internal endothelium.
Results: Among 187 tumors 114 tumors showed higher and 73 tumors lower actinin-4 expression. Actinin-4 intensity was correlated with location (p=0.012), mitosis (p=0.022), MIB-1 score (p=0.002), tumor grade (p=0.013), and GIST risk classification (p=0.008), but not with size, histology (epithelioid vs spindle), nectosis, and clinical outcome.
Conclusions: Actinin-4 staining was associated with tumor grade and GIST risk classification and can be helpful in management of patients with these tumors.

76 Frequency and Characterization of *ATF1*-Fusion Genes in Angiomatoid Fibrous Histiocytoma

SBSP Terra, AL Folpe, SW Weiss, AG Nascimento, MR Erickson-Johnson, X Wang, AM Oliveira. Mayo Clinic, Rochester, MN; Emory University, Atlanta, GA.
Background: Angiomatoid fibrous histiocytoma (AFH) is a rare soft tissue tumor of borderline malignancy and uncertain line of differentiation. A very small number of AFH has very recently been shown to harbor rearrangements of the cAMP-dependent transcriptional factor *ATF1*, first with *FUS* and more recently with the closely related gene, *EWSR1*. We performed molecular cytogenetic analysis of 14 cases of AFH using fluorescence in situ hybridization (FISH) to determine the frequency and nature of the *ATF1*-fusion genes in these tumors.
Design: Fourteen cases of AFH with classic histologic features diagnosed in patients between 3 and 52 years were studied in these series. *ATF1*, *FUS* and *EWSR1* gene rearrangements were evaluated by fluorescence in situ hybridization (FISH) using custom designed and commercially available probes for paraffin-embedded thin tissue sections. Approximately 400 cells were analyzed in each tumor by three independent investigators.
Results: Four (of 14) cases (29%) showed *ATF1* rearrangements in between 25 and 80% of the cells. Three AFH contained *EWSR1-ATF1* fusion genes; the remaining case harbored a *FUS-ATF1* fusion gene. No association between age, tumor size, anatomic location, or desmin expression and the presence of *ATF1*-fusion genes was found. Interestingly, all positive cases occurred in female patients. The non-neoplastic chronic inflammatory cells found at the periphery of all cases served as internal controls, and showed no molecular cytogenetic abnormalities.
Conclusions: We have found that *ATF1*-fusion genes occur in approximately one third of histologically classic AFH. Interestingly, in this series the more recently described *EWSR1-ATF1* fusion gene was three times more common than the *FUS-ATF1*. The presence of genetic abnormalities appears to be independent of other clinicopathological parameters in AFH, although any possible prognostic value of these fusion genes remain to be determined. The absence of *ATF1*-fusion genes in two thirds of cases also indicate the presence of alternative oncogenic mechanisms in AFH.

77 Molecular Diagnosis of Primitive Neuro-Ectodermal Tumor/Ewing Sarcoma (PNET/ES): Comparision of RT-PCR and FISH. A Study of 104 Cases

R Tirabosco, TC Diss, K Bousdras, AM Flanagan. Royal National Orthopaedic Hospital, Stanmore, United Kingdom; University College London, London, United Kingdom; University College Hospital, London.
Background: RT-PCR and FISH are widely employed in the diagnosis of tumors bearing specific chromosomal translocations. PNET/ES are a group of tumors characterized by translocations involving the EWS gene. The aim of this study was to determine how many of the bone and soft tissue tumors diagnosed in our Institution as PNET/ES on the basis of morphology and immunohistochemistry harbored a EWS gene rearrangement.
Design: Between March '03 and April '06, 123 PNET/ES were diagnosed. Selection criteria included primary tumors, where paraffin-embedded material was available for molecular analysis, which were radiologically and immuno-morphologically consistent with PNET/ES. 85 cases fulfilled these criteria. The total number of cases analyzed was brought to 104 by including an additional 19 cases prior to 2003: this permitted assessment of the suitability of archival tissue for molecular studies. RNA was extracted using a commercial kit. Conventional RT-PCR, and dual-color FISH were performed using manufacturers' protocols.
Results: The patients' age ranged from 1-65 years: 83% presented before the age of 30. 72(69%) cases arose in bone and 32 (31%) in soft tissue. Of the 104 cases analyzed by RT-PCR, amplifiable RNA was obtained in 88 (85%). A EWS fusion gene was detected in 76 cases (73%): the detection rate was similar in bone and soft tissue lesions (72% vs 75%, respectively). The relative frequency of EWS transcript types and variants was in keeping with published data. All but one of the 31 randomly selected tumours from the 76 RT-PCR-positive cases were also positive by FISH (97% concordance). In addition, of the 28 RT-PCR negative cases, 18 were found to be positive by FISH, which brought the total number of cases that harbored a EWS gene rearrangement to 94 (90.3%). Results from the archival material gave similar results to those of the more recent material.
Conclusions: The protocols employed in this molecular study using paraffin-embedded tissue, the largest of its kind to date from a single Institution, of PNET/ES shows that FISH is a more useful and less labor-demanding technique for provision of a rapid diagnostic service than RT-PCR. In FISH-negative cases, or when a specific transcript is sought for research purposes, then more sophisticated but labor-intensive RT-PCR is an alternative approach as this may increase the gene rearrangement detection rate.

78 Fluorescence In Situ Hybridization (FISH) for MDM2 Gene Amplification in Formalin-Fixed Paraffin-Embedded Tissue (FFPET) as a Diagnostic Tool in Lipomatous Neoplasms

J Weaver, E Downs-Kelly, RR Tubbs, JR Goldblum, S Turner, M Skacel. Cleveland Clinic, Cleveland, OH.
Background: Well-differentiated liposarcomas/atypical lipomatous tumors (WDLS/ALT) and dedifferentiated liposarcomas (DDLS) can be difficult to distinguish from benign lipomatous neoplasms and other high-grade sarcomas (HGS), respectively. Cytogenetics has identified ring and giant chromosomes throughout the spectrum of WDLS/ALT and DDLS, composed of 12q13-15 amplicons with resultant amplification of the *MDM2* gene. Demonstration of *MDM2* amplification by FISH in FFPET could be an adjunctive tool in the differential diagnosis of WDLS/ALT and DDLS and may prove especially useful as the prevalence of needle biopsy for diagnosis increases.
Design: FISH for *MDM2* amplification was performed on FFPET whole sections from WDLS/ALT (n=14), DDLS (n=14), spindle cell/pleomorphic lipomas (SC/PL; n=9), angiolipomas (n=5), and lipomas (n=4) and on a FFPET tissue microarray (TMA)

containing a variety of soft tissue neoplasms. The assay employs probes specific for *MDM2* (12q15, Vysis®) and the centromere of chromosome 12 (*CEP12,* Vysis®). After counting signals from 40 nuclei/case we calculated a *MDM2/CEP12* ratio; a ratio >2.0 was considered amplified, ≤2.0 non-amplified, and ~1 with >2 signals of both probes polysomy for *CEP12*.

Results: 96.4% of WDLS/ALT and DDLS showed amplification of *MDM2* (mean: >17 copies/nucleus; *MDM2/CEP12* ratio: 7.5), with amplification in both the atypical and cytologically unremarkable cells, and the degree of amplification correlating to the degree of cytologic atypia. *CEP12* polysomy was noted in 8/9 (88.9%) SC/PL (*MDM2/CEP12* ratio: 0.97). All angiolipomas and lipomas were non-amplified (*MDM2/CEP12* ratio: 1). 1/1 epithelioid sarcoma, 1/4 malignant peripheral nerve sheath tumors, and 1/5 myxoid liposarcomas showed *MDM2* amplification. All other soft tissue neoplasms were non-amplified.

Conclusions: The *MDM2/CEP12* FISH assay is a sensitive and specific tool (93% and 100%, respectively) for evaluating atypical lipomatous neoplasms. The specificity decreases when evaluating HGS, since *MDM2* amplification was seen in a subset of HGS other than DDLS. In most instances, these other HGS can be distinguished from DDLS by their immunohistochemical profile or characteristic translocation (i.e. t(12;16) involving CHOP in MLS). No benign lipomatous lesions were *MDM2* amplified and the non-atypical cells in WDLS were positive, making the probe a valuable diagnostic tool in the differential diagnosis of WDLS/ALT and DDLS.

79 D2-40 (Podoplanin) Is a Novel Marker for Follicular Dendritic Cell Sarcoma

H Yu, JA Gibson, GS Pinkus, JL Hornick. Brigham and Women's Hospital, Harvard Medical School, Boston, MA.

Background: Podoplanin is a membrane glycoprotein expressed in a variety of human cell types, including glomerular epithelium, lymphatic endothelium, and mesothelium. Recent studies have demonstrated the utility of podoplanin (recognized by monoclonal antibody D2-40) in the diagnosis of mesothelioma and seminoma. In the course of evaluating clinical cases, we observed that follicular dendritic cells (FDC) within lymphoid follicles are strongly positive for D2-40. However, podoplanin expression in FDC sarcomas has not previously been examined. The purpose of this study was to evaluate the expression and specificity of podoplanin in FDC sarcomas compared to other spindle cell sarcomas.

Design: 80 tumors were studied: 11 FDC sarcomas; 29 gastrointestinal stromal tumors (GIST), including 13 spindle cell, 7 epithelioid, and 9 mixed type; and 10 cases each of malignant peripheral nerve sheath tumor (MPNST), leiomyosarcoma, monophasic synovial sarcoma, and solitary fibrous tumor (SFT). Immunohistochemical studies were performed following epitope retrieval (0.01M citrate buffer, pH 6.0; pressure cooker) using monoclonal antibody D2-40 (Signet Labs) and an EnVision+ peroxidase detection system (Dako). The extent of immunoreactivity was graded according to the percentage of positive tumor cells: 0, <5%; 1+, 5-25%; 2+, 26-50%; 3+, 51-75%; and 4+, 76-100%; and the intensity of staining was graded as weak, moderate, or strong.

Results: All FDC sarcomas (100%) showed moderate or strong immunoreactivity for D2-40 (4+ [5], 3+ [2], 2+ [4]). D2-40 expression was only occasionally observed in the other tumor types examined: 7 (24%) GISTs (4+ [1], 3+ [3], 2+ [1], 1+ [2]), 3 (30%) synovial sarcomas (3+ [1], 2+ [1], 1+ [1]), 1 (10%) MPNST (1+), 1 (10%) leiomyosarcoma (3+), and 0 (0%) SFT. Interestingly, immunoreactivity for D2-40 was more common in spindle cell GISTs (38%) than in epithelioid or mixed-type GISTs (13%). In contrast to FDC sarcomas, the intensity of staining for D2-40 was weak in all but 5 of the other positive tumors.

Conclusions: Podoplanin is a highly sensitive marker for FDC sarcoma and may be useful in a panel for characterization of these unusual tumors. However, a subset of GISTs (in particular, spindle cell type) is also positive for D2-40, and limited podoplanin expression may occasionally be detected in other spindle cell sarcomas.

Breast

80 Morphological and Molecular Evolutionary Pathways of Low Grade Breast Cancers and Their Putative Precursor Lesions

T Abdel-Fatah, DG Powe, Z Hodi, JS Reis-Filho, A Lee, IO Ellis. Nottingham University, Nottingham, United Kingdom; Institute of Cancer Research, London, United Kingdom.

Background: We investigated the morphological and molecular evolutionary pathways involved in the development of low grade breast cancers by studying the frequency of association and immunoprofile of putative precursor lesions including CCLs, UEH, ADH, DCIS, and LN.

Design: The frequency of invasive and pre-invasive lesions was microscopically determined in 200 low grade breast tumours comprising low grade IDC, cribriform, pure and mixed type tubular (TC), tubulolobular (TLC) and ILC classic type. Tissue microarrays containing 1100 of these lesions were immunohistochemically compared for putative tumour suppressor genes (TSGs), cell cycle regulators, proliferation and differentiation markers.

Results: Morphology: > 85% low grade IDC, cribriform, TC and TLC had associated CCLs with the majority showing flat epithelial atypia (FEA). CCL, DCIS and invasive lesions co-localized in >80% patients; LN occured in only 16% cases compared to 91% ILCs. Immunohistochemistry: Epithelial cells in the putative precursor FEA, ADH, LN, DCIS lesions and associated cancers were negative for basal/ myoepithelial markers but positive for CK19/18/8, ER-α, Bcl-2, and Cyclin D-1. Contiguous cells expressing ER-α increased in columnar cell hyperplasia (CCH), rising with atypia. ER-α/ER-βratio and Cyclin D-1 expression increased during carcinogenesis. Bcl-2 was frequent in epithelial cells lining CCLs, ADH, LN and low grade DCIS compared to associated carcinoma. FHIT and ATM expression was reduced in hyperplastic CCLs, ADH/DCIS, LN and associated invasive lesions.

Conclusions: We suggest that CCLs, particularly FEA, are common in low grade breast carcinoma and ILC, representing a family of precursor, *in situ* and invasive neoplastic lesions belonging to the luminal 'A' subclass. Our results suggest that the committed progenitor cells for low grade breast neoplasia are CK19/18/8+, ER-α and Bcl-2+. The balance between ER-α/ER-β expression may be important in driving cyclin D-1 and Bcl-2 expression. Alternatively, 'breast cancer stem/ progenitor cells' regardless of their original phenotype acquire early stochastic genetic/epigenetic hits, leading to activation of the luminal A pathway (ER/cyclin D1 pathways) that determine the phenotype of pre-invasive and invasive lesions. We speculate that once cells commit to this 'molecular pathway', progression to a 'high grade' (basal-like or HER2) phenotype would be unlikely.

81 Intra- and Peritumoral Lymphatic Vessel Density in Breast Cancer: Correlation with Clinicopathologic Features and Prognostic Significance

G Acs, X Xu, T Pasha, PJ Zhang. H. Lee Moffitt Cancer Center, Tampa, FL; University of Pennsylvania Medical Center, Philadelphia, PA.

Background: The earliest feature of disseminated disease in breast cancer is regional lymph node involvement. Despite its major role in tumor dissemination, little is known about the interaction of tumor cells with lympahtic vessels, the role of tumor lymphangiogenesis in the metastatic process and whether lymphatic spread occurs via pre-existing lymphatics or vessels newly formed by lymphangiogenesis. The monoclonal antibody D2-40 detects a fixation-resistant epitope on podoplanin and has been shown to be a selective marker for lymphatic endothelium useful in specifically identifying lymphatic vessels in malignant neoplasms.

Design: We examined the intra- and peritumor lymphatic vessel density (LVD) in a series of 256 pT1 and pT2 invasive breast carcinomas using D2-40 immunohistochemistry on formalin-fixed paraffin-embedded tissue sections. The lymphatic density within the tumors (intratumor LVD, ILVD) and within 2 mm of the edge of tumors (peritumor LVD, PLVD) was determined in 5 high power fields (X200) withy the highest number of D2-40 positive lymphatic vessels. The ILVD and PLVD was correlated with clinicopathologic tumor features, the extent of retraction artifact around tumor cell nests and patient outcome.

Results: Intra- and peritumoral lymphatic vessels were detected in 116 (45%) and 249 (97%) tumors, respectively. Peritumor LVD (5.64 ± 0.28, mean ± SEM) was significantly higher compared to intratumor LVD (0.86 ± 0.11) ($p < 0.0001$). High intra- and peritumor LVD showed significant correlation with tumor grade, tumor size, presence of lymphatic invasion, nodal metastasis, extensive retraction artifact around tumor cell nests and presence of D2-40 immunoreactivity in tumor stroma. High intra- and peritumor LVD was highly significantly associated with poor recurrence-free and overall survival in univariate analysis. In multivariate analysis, high peritumor LVD remained an independent factor predicting poor recurrence-free survival.

Conclusions: High density of both intra- and peritumor lymphatic vessels in breast carcinomas are associated with more advanced, agressive diasease and poor outcome, suggesting that tumor associated lymphangiogenesis may play an important role in the progression of breast cancer. Determination of LVD may serve as a prognostic and/or predictive factor in breast cancers.

82 Effect of Preoperative Chemotherapy (PCT) on Locally Advanced Breast Cancer (LABC) among Mexican Women

I Alvarado-Cabrero, M Patiño, A Hernandez, S Barroso, E Ruiz. Mexican Oncology Hospital, Mexico, DF, Mexico.

Background: Preoperative chemotherapy (PCT) is a therapeutic option for locally advanced breast cancer(LABC). Pathological assessment of response to PCT in each patient could be use as an in vivo method to assess chemotherapy sensitivity. **Goals**: To evaluate the effects of chemotherapy(CT) on breast cancer tissue and to know the factors that can influence in the pathologic response.

Design: Between july 2000 and june 2003, 135 patients presented to the Hospital with LABC. All patients had a biopsy proven diagnosis of breast carcinoma. Chemotherapy consisted of 4-6 cycles of preoperative FEC, followed by mastectomy with axillary lymph node dissection(ALND). A complete pathologic response(PCR) was defined as the absence of any microscopic evidence of tumor in the mastectomy specimen and ALND. Noncomplete pathologic response(NPR) was defined as having invasive carcinoma at excision. Immunohistochemical stainings(estrogen receptor(ER), progesterone receptor(PR) and c-erB-2) were performed on 135 pretherapeutical specimens. Fisher´s exact test was used for statistical analysis.

Results: The patient's ages ranged from 24 to 79years with a mean age of 54 years. Eleven of the 135(8%) patients had a PCR while 3(2%) patients had microscopic residual disease in lymph nodes. Patient age failed to predict the clinical or pathologic response of breast tumors(P: 0.8). The mean tumor size was 6cm; initial tumor size was not a predictor of PCR(P: 0.6). Of the 135 invasive carcinomas, 90(67%) were ductal(IDC), 31(23%) lobular (ILC), 12(9%) pure micropapillary carcinoma (IMPC) and 2(1.4%) mucinous carcinoma. Thirty five(42%) IDC diagnosed on the biopsy turned out to have two or three types of tumor.(eg.tubular)in the mastectomy specimen. Seventy nine of the cases were grade II and 56 grade III. Patients with a PCR had initial tumors that were more likely to be anaplastic(P:0.3). A PCR was predictive of a axillary lymph node response(P: 0.1). IMPC had a high incidence of ALNMetastases (m:11, Lymph nodes). ER, PR, and Her-2/neu expression was not associated with response to PCT.

Conclusions: PCR among Mexican patiens with LABD is low(8%) High incidence of ILC, no cases of local response IMPC is an aggressive tumor resistant to conventional CT.